*sustainability*

MDPI

*Article*

# Advancing Sustainability in Surface Coal Mines Through Real-Time Air Quality Monitoring: Low-Cost IoT Solutions and the Role of Meteorological Factors in PM and GHG Emissions

**Vislavath Suresh [1], Siddhartha Agarwal [1,*], Yoginder P. Chugh [2], Priyanshu Jha [1] and Renzhong Wang [3]**

[1] Department of Mining Engineering, Indian Institute of Technology (ISM), Dhanbad 826004, India; 21dr0217@me.iitism.ac.in (V.S.); 20je0725@me.iitism.ac.in (P.J.)
[2] College of Engineering, Computing, Technology and Mathematics, Southern Illinois University, Carbondale, IL 62901, USA; siu681@siu.edu
[3] Microsoft Corporation, Redmond, WA 98052, USA; rewan@microsoft.com
* Correspondence: sagarwal@iitism.ac.in

**Abstract:** This paper presents a development of a "smart center" for studying particulate matter (PM) and other gaseous emissions pollution in a surface coal mine located in the Jharia coalfield of Jharkhand, India, utilizing internet of things (IOT)-based capabilities and low-cost sensors data. These pollutants in the air in and around surface mines present significant environmental challenges that require comprehensive assessment and management. This study undertook four winter months from January to April 2023 of real-time, low-cost IoT-based monitoring of $PM_1$, $PM_{2.5}$, $PM_{10}$, $SO_2$, $NO_2$, $O_3$, CO, $CO_2$, TVOC, and noise pollution, along with meteorological parameters, such as humidity, rainfall, and temperature. Data were collected at three locations: within a mine site area, in a buffer zone located 1.5 km from the mine, and at a non-impacted residential area within the university campus. Mining operations and active mine fires are primary contributors to pollution. Peak PM concentrations around the mining site were observed during morning and evening hours (5–7 a.m. and 4–6 p.m.). This study further identified that air pollutant concentrations were positively correlated with humidity but negatively correlated with the atmospheric temperature at the mine site, but not at the university campus of the IIT–ISM.

**Keywords:** particulate emissions; GHG; coal mines; air quality sensors; IoT-based monitoring

check for updates

Academic Editors: Peng-Yeng Yin and Reza Daneshazarian

Received: 19 October 2024
Revised: 17 December 2024
Accepted: 17 January 2025
Published: 5 February 2025

**Citation:** Suresh, V.; Agarwal, S.; Chugh, Y.P.; Jha, P.; Wang, R. Advancing Sustainability in Surface Coal Mines Through Real-Time Air Quality Monitoring: Low-Cost IoT Solutions and the Role of Meteorological Factors in PM and GHG Emissions. *Sustainability* **2025**, *17*, 1301. https://doi.org/10.3390/su17031301

**Copyright:** © 2025 by the authors. Licensee MDPI, Basel, Switzerland. This article is an open access article distributed under the terms and conditions of the Creative Commons Attribution (CC BY) license (https://creativecommons.org/licenses/by/4.0/).

## 1. Introduction

India is the world's third-largest energy consumer, with coal accounting for about 55% of its energy needs [1]. The country's energy demand has doubled since 2000, driven by rising incomes, urbanization, infrastructure, job creation, and energy security, and efforts to reduce coking coal imports from Indonesia, Australia and other countries [2,3]. Thus, the Ministry of Coal for the Government of India has prioritized domestic production, achieving a 57.87% increase to reach 893.19 million metric tons (MT) for the fiscal year 2022–2023, from 565.77 MT in 2013–2014. The production is expected to reach a billion tons in 2023–2024 [4].

Open pit mines in India currently account for about 95% of the coal production (Annual report 2023–2024, Ministry of Coal), which has resulted in a significant increase in coal mining activities, particularly in surface coal mines [5]. These activities, have resulted in substantial environmental challenges, including the emission of particulate matter (PM) and gasesous emissions and greenhouse gases (GHGs) [6] Monitoring and managing these

emissions are critical to mitigating their adverse effects on air quality, climate change, and public health [7,8].

The mining process includes excavating large tracts of land, which releases dust, particulate matter (PM) [9], greenhouse gases (GHG's) and volatile organic compounds (VOC's) into the air [10–12]. Subsequent Other major coal mining operations, such as drilling and blasting [13,14], transportation of coal and overburden [15], loading and unloading of dumpers [16], and coal mine fires due to spontaneous heating [17], also produce substantial amounts of PM and other noxious gases. However, the extraction and combustion of coal are the primary sources of air pollution in surface coal mines [18,19]. According to estimates by [20], over 25% of all coal dust is emitted during the loading and unloading of transport vehicles, and roughly 50% occurs during driving on unpaved haul roads. Road transport over unpaved roads and dust from exposed overburden dumps, coal handling plants, and exposed mining faces have been identified as the main source of total suspended particles (TSP) and $PM_{10}$ pollution [21,22]. Drilling and blasting [13] are the other next important sources of fugitive, dust along with wind erosion from coal stockpiles [15]. Spontaneous combustion [17] of coal and uncontrolled fires in the Indian mines of Jharia are a major source of pollution [23]. Other air pollution sources include diesel emissions from heavy earth moving machinery (HEMM) used in opencast mining, such as bulldozers, excavators, and trucks [24]. Natural sources of air pollution around opencast mines in India include wind-blown dust, vegetation fires, surface and underground coal mine fires, and other natural events [25].

Prolonged exposure to elevated levels of particulate matter can have a negative impact on the health of people residing in the surrounding areas by causing respiratory disorders [26,27], cardiovascular problems, and other related diseases [28–30]. In addition to health risks, air pollution from surface coal mines can also alters the regional climate and intensify climate change worldwide [31]. Greenhouse gas emissions, particularly $CO_2$ and methane, play a key role in global temperature rise, resulting in melting ice caps, increasing sea levels, and extreme weather conditions [32].

Conventional methods of monitoring air quality in coal mines have used on the manual sampling and laboratory analysis of those samples [33]. Despite offering accurate data, these conventional methods are time consuming and lack real-time capabilities. The shortcomings of conventional methods underscore the need for more effective and instantaneous monitoring systems [34]. Therefore, there is an increasing interest in adopting emerging technologies, such as artificial intelligence (AI) and the internet Of things (IoT) for environmental monitoring. IoT devices equipped with various sensors can continuously collect data on air quality, temperature, humidity, and other environmental parameters [35].

Recent research has shown how the IoT and AI-based technologies have been used in industrial environments to monitor air quality. For example, research in China that monitored methane emissions in coal mines using IoT sensors and AI algorithms saw a substantial decline in emissions [36]. Similarly, another study in Australia of an IoT based dust level monitoring system that was used in a surface mine resulted in improved air quality management and adherence to environmental regulations [37]. In India, Sharma and Kumar (2023) [38] demonstrated the usefulness of employing IoT-enabled sensors to monitor air quality in surface coal mines, emphasizing the necessity of long-term air quality initiatives.

IoT and AI-based monitoring systems have a lot of potential, but there are also numerous obstacles to overcome, which include high upfront expenses [39], the requirement for qualified staff to oversee and maintain the systems [40], the technological difficulties [41], and the data security issues [42]. However, the potential of IoT and AI for accurate data, cost-effectiveness, and real-time monitoring highlights the need for additional research.

To overcome these obstacles, the creation of a smart center that is based on the IoT and AI, which is especially intended for air quality monitoring in surface coal mines, has been proposed. The goal of the developed smart center is to provide real-time data collection, processing, and reporting, to facilitate proactive steps to lower emissions and enhance environmental sustainability.

This paper aims to describe an internet of things (IoT) based smart system designed for monitoring ambient air quality. Additionally, it presents a cloud-based data analysis module that examines various particulate matter (PM) pollutants and their dependencies on daily atmospheric variations, such as temperature and humidity, specifically for surface coal mines. Data for this study were collected using low-cost sensors housed in a single box, with one-minute sampling interval, from January 2023 to May 2023 (Figure 1). The monitoring network comprised three locations: the industrial zone (surface coal mine), the buffer zone (mining GM office (HQ) and residential colony) 1.5 km from the mine, and the IIT campus 12 km from the mine. Data were collected to measure the concentrations of different air pollutants in real time. The collected data were used for trend analysis and to identify pollution hotspots.

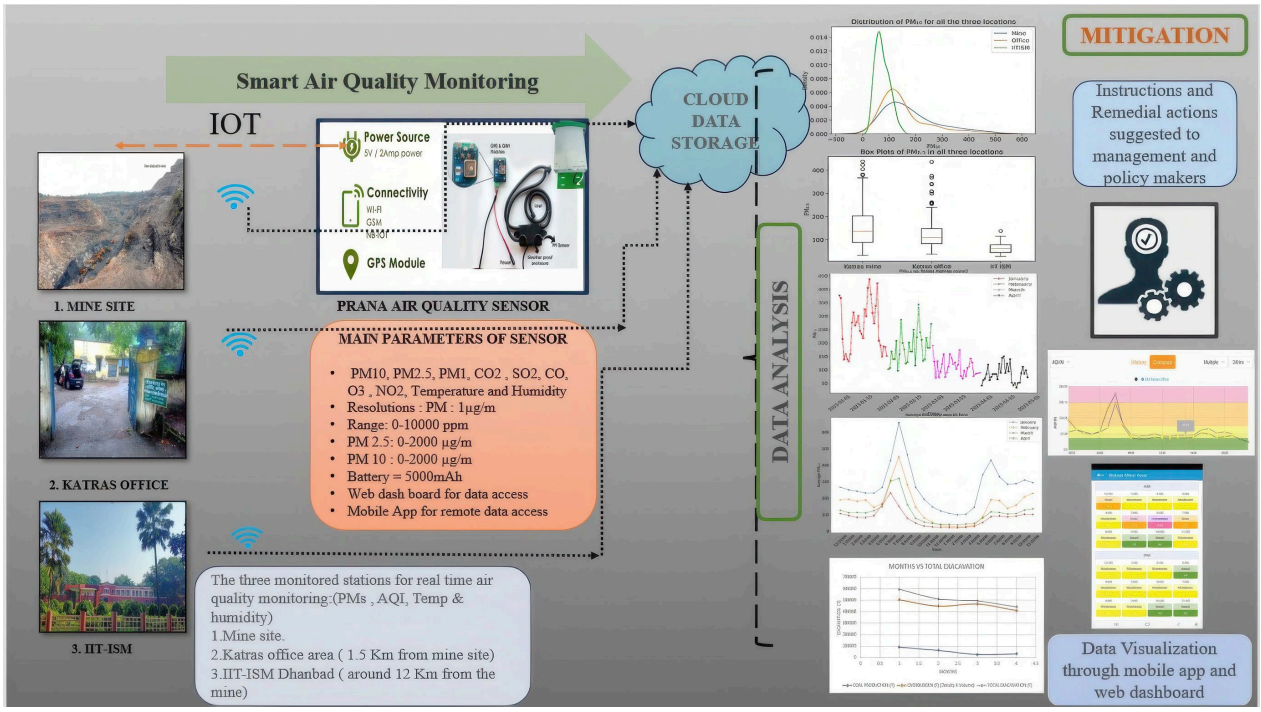


**Figure 1.** Graphical abstract of the research.

This research contributes significantly to sustainability through socio-economic, scientific, and integrated approaches. By enabling real-time air quality monitoring, this study addresses worker health and safety and GHGs emissions. Healthier workers result in reduced medical costs and improved productivity, reinforcing the importance of proactive environmental monitoring. The use of low-cost IoT sensors also ensures cost-effective air-quality management, making these systems accessible to smaller mines in developing regions and fostering widespread adoption of air quality management practices. This affordability contributes to long-term savings in pollution control and regulatory compliance.

## 2. Study Area

The research was conducted at an open pit mine in the Jharia coalfields of India near the Dhanbad city. The mine began operations in 1990 and currently has a depth

of 100 m [43]. Five coal benches and seven overburden (OB) benches are currently in operation. The mine's leasehold area is 717.80 hectares, of which 280 thousand sq. meters of area is affected by fire due to spontaneous coal combustion. The production of coal and overburden in the mine from January 2023 to April 2023 is shown in Table 1. As part of the research, three regions, namely industrial, buffer, and sensitive, were identified to determine the effect of mining activities on air pollution levels in and around the region. The first monitoring station was positioned at the mine site to represent the industrial zone. The remaining two stations include a buffer zone: the mine general manager's office (headquarters) and village residents, located 1.5 km from the mine site. The third monitoring station was positioned at the Mining Engineering Indian Institute of Technology (Indian School of Mines), Dhanbad, which has a green college campus with student hostels and professors' residences 12 km from the mine site. The location of monitoring points in aerial view is shown in Figure 2. The red line indicates the administrative boundaries between Baghmara—cum Katras block (tehsil) and Dhanbad cum Kenduadih cum Jagda block (tehsil) of Dhanbad where stations a and b lie in Baghmara—cum Katras block (tehsil) and station c lie in Dhanbad cum Kenduadih cum Jagda block (tehsil) of Dhanbad. The view of the monitoring air quality stations for all three sites is shown in Figure 3. These locations lie in a transitional zone between a humid subtropical climate and a tropical wet and dry climate. From November to early March, the weather remains cold, with temperatures ranging from a minimum of 10 °C to a maximum of 22 °C. From the last week of March to June, the weather turns hot, with temperatures varying from 25 °C to a maximum of 47 °C. During this period, the average wind speed is 10.3 km/h, with the dominant wind direction being northwest.

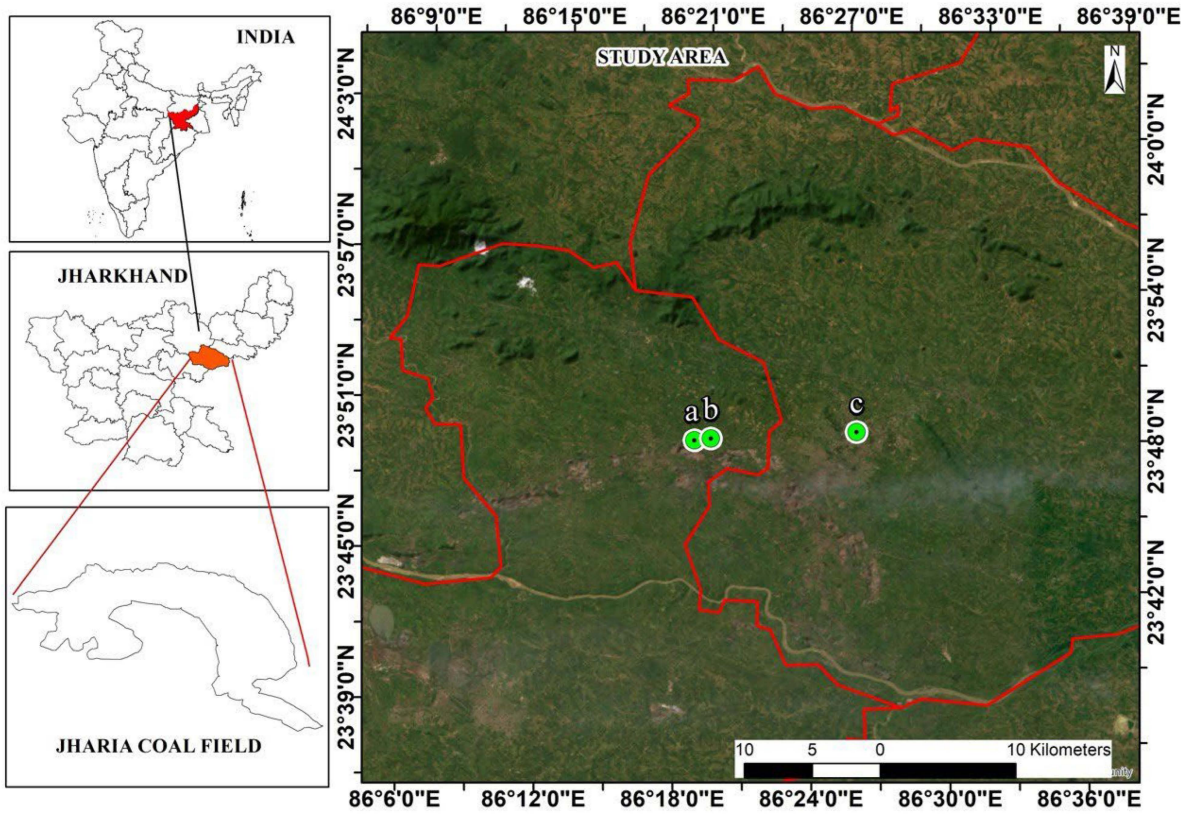


**Figure 2.** Map showing the location of monitoring stations. (a) Mine site (23°48′43.3″ N, 86°19′29.3″ E). (b) Mine GM office (HQ) (23°48′46.1″ N, 86°20′12.6″ E). (c) IIT–ISM Dhanbad (23°48′47.88″ N, 86°26′30.84″ E).




(**a**) Mine site (23°48′43.3″ N, 86°19′29.3″ E)



(**b**) Mine GM office (HQ) (23°48′46.1″ N, 86°20′12.6″ E)



(**c**) IIT–ISM Dhanbad (23°48′47.88″ N, 86°26′ 30.84″ E)

**Figure 3.** Photographs of sensor monitoring station deployed in (**a**) mine site, (**b**) mine GM office (HQ), 1.5 km from the mine, and (**c**) IIT–ISM Dhanbad, which is around 12 km from the mine site with geographical coordinates respectively.

**Table 1.** Production of coal and overburden in mine from January 2023 to April 2023.

| Months | Coal Production (T) | Overburden ($M^3$) | Overburden (T) (Density × Volume) | Total Excavation (T) |
|---|---|---|---|---|
| January | 91,875 | 230,471 | 502,426.8 | 594,301.8 |
| February | 63,735 | 205,340 | 447,641.2 | 511,376.2 |
| March | 26,965 | 213,991 | 466,500.4 | 493,465.4 |
| April | 32,909 | 187,735 | 409,262.3 | 442,171.3 |

## 3. Methodology

This study used a real-time air quality monitoring system (RTAQMS). This system operates digitally and provides real-time air quality data. The system has various sensors [44] to detect $PM_{10}$, $PM_{2.5}$, and $PM_1$ and count the number of particles, along with measuring gases such as $O_3$, $CO_2$, CO, $SO_x$, $NO_x$, V OC, as well as temperature, and humidity. Please refer to Table A1 in Appendix A for the list of main parameters of air quality monitoring sensors and their respective range, resolution, and accuracy.

### *3.1. Working Principle of the IoT Devices and Sensors*

Air quality was assessed using the Prana C-Air Plus air quality monitor (Prana Air, New Delhi, India). The low-cost sensors detect PM using the optical 90° light scattering principle, as shown in Figure 4. They feature a built-in laser and photoelectric receiving module. When light strikes the mirror aperture at 90°, it is reflected towards the sensor [45]. The photodiode registers a pulse as long as the light is reflected. The received electrical signal is then converted into the concentration of particulate matter using specific algorithms [46]. The sensors were deployed at all three selected sites in open spaces with minimal obstructions and powered by a 220 V power supply. Since PM distribution is influenced by wind speed and direction, an average of PM readings from multiple directions was considered. Real-time levels of various pollutants can be viewed through a web dashboard and mobile application. The sensors' printed circuit boards (PCBs) can be connected using various communication modes, such as UART (universal asynchronous receiver/transmitter), Wi-Fi, RS-485, and GSM (global system for mobile communication), offering flexibility and compatibility with diverse systems and devices. The sensors were carefully selected to balance quality and cost, aiming to accurately calculate the air quality index (AQI) level.

The parameters were measured over four months, from January to April 2023. This period covers winter and early spring, allowing for observing seasonal changes in air quality, including the impact of heating in winter and the onset of warmer weather. The four-month period was chosen to capture key seasonal transitions, including winter heating effects and early spring changes in air quality. While a longer study would provide more comprehensive insights, resource constraints limited the study duration. We plan to extend the timeline in future studies for broader seasonal coverage.

The system uses air sensors to detect and transmit data to the microcontroller. The microcontroller then stores this data on the web server [47]. The processor analyzes the information from the web server and forwards the processed data to the predictor, which anticipates the presence of hazardous air particles. Thus, integrating IoT devices and sensors makes monitoring toxic air particles straightforward, as illustrated in Figure 4. Routine maintenance of the low-cost sensors involves cleaning the sensors to prevent dust accumulation, which could affect their accuracy. The sensors were inspected regularly for any physical damage or malfunction, and any issues detected were promptly addressed to minimize data errors.

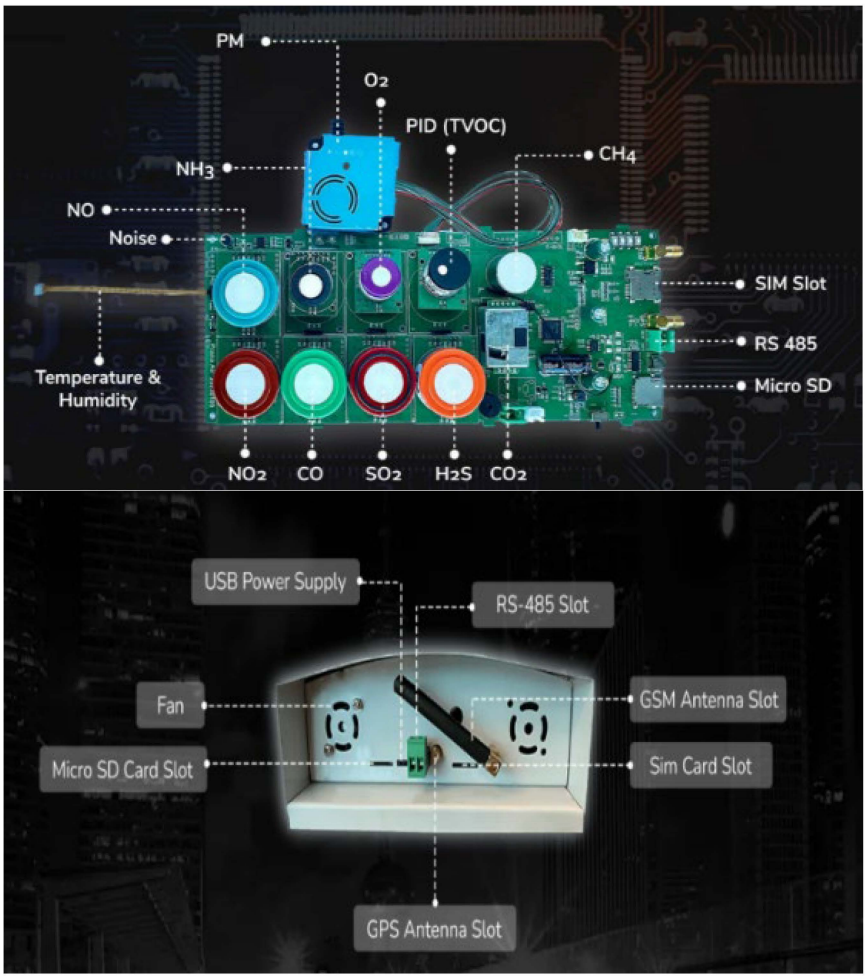


**Figure 4.** Air Quality Monitoring System and its parts (source: pranaair.com).

### *3.2. Data Collection, Storage, and Management*

Real-time data on various air quality and metrological parameters, as discussed in previous sections [48], are systematically gathered by strategically positioning IoT devices at three different locations. The collected data is then transmitted to a centralized system, which undergoes secure storage, as shown in Figure 5. This storage infrastructure is designed to efficiently handle the substantial volume of real-time data generated by the IoT devices. Advanced data management techniques, possibly including cloud-based solutions, are employed to organize and catalogue the information for easy retrieval and analysis. The implementation of the IoT in this context offers several advantages. It enables prompt detection of fluctuations in air quality, facilitating timely responses to potential issues [49]. Additionally, the continuous and automated nature of data collection through IoT devices reduces the reliance on manual methods, minimizing the risk of human error, and ensuring a more comprehensive and accurate dataset. In Figure 6, the flowchart outlines the data collection, analysis, and action-taking process using IoT sensors after data analysis. The flow then splits into two paths: one leading to real-time data analysis and the other to historical data logging. Real-time data analysis triggers instant alerts and notifications in case of abnormal air quality conditions, ensuring swift responses. If specific threshold values are met, an alarm/notification is given to associated management, and recommended remedial measures are suggested to supervisors. If the threshold value is not met, the process ends. Simultaneously, historical data logging facilitates long-term trend analysis and regulatory compliance reporting.

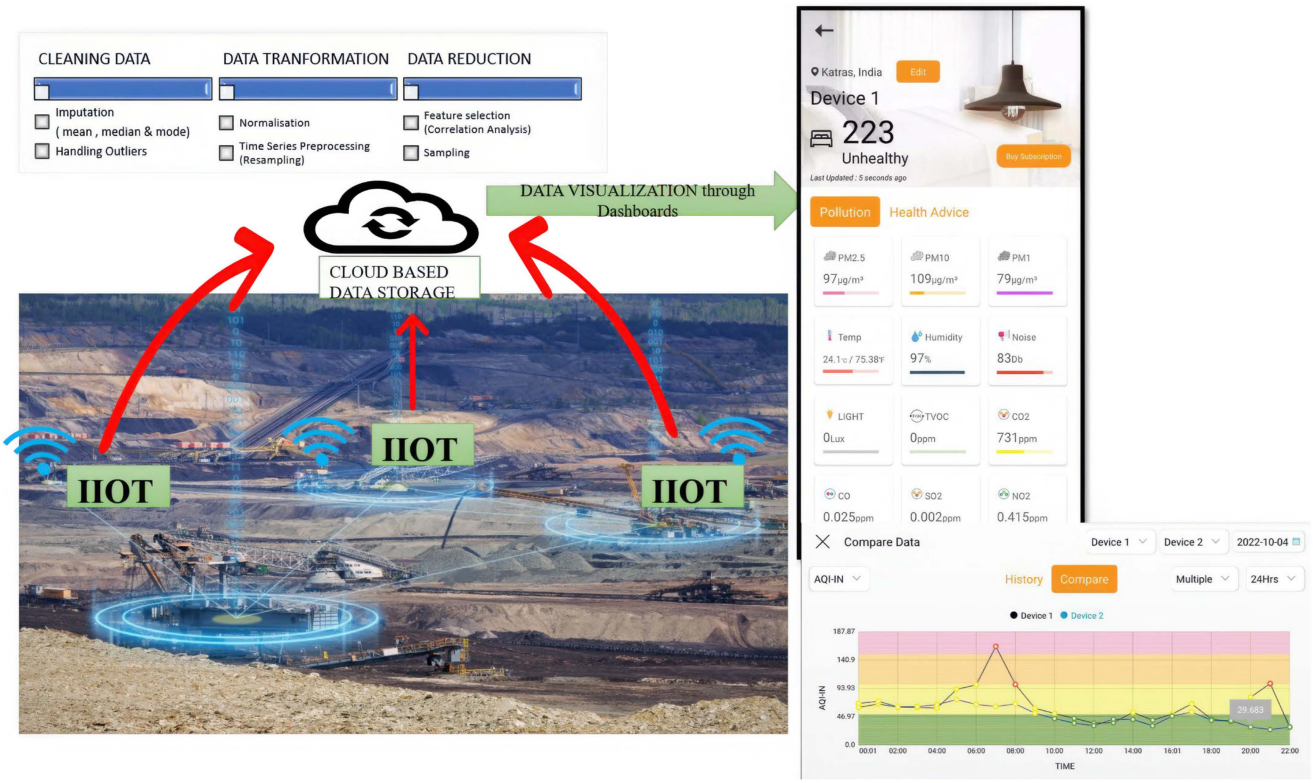


**Figure 5.** Overview of IoT-based monitoring of air pollution and data acquisition in open-pit mines.

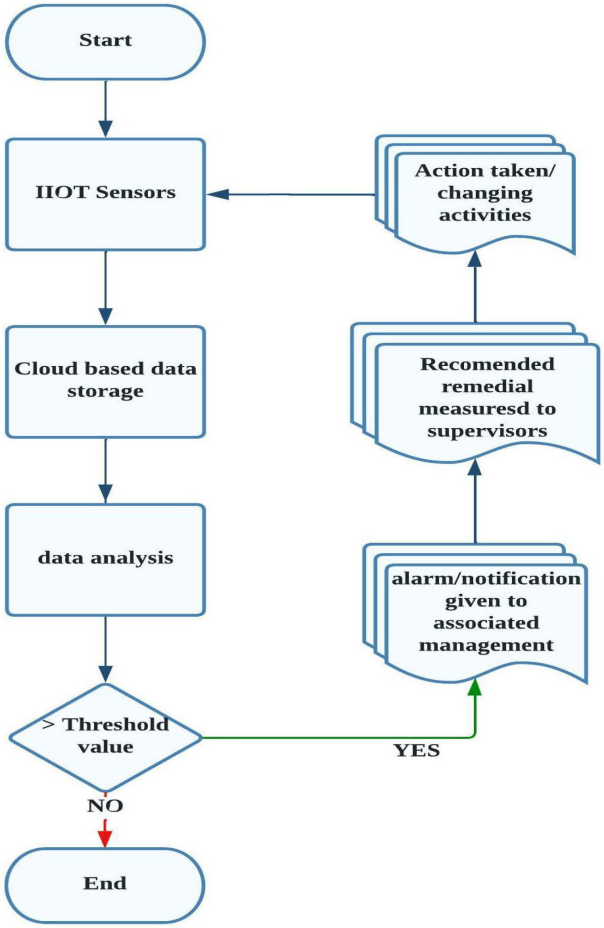


**Figure 6.** Proposed flow chart for this study.

### *3.3. Data Pre-Processing*

The data pre-processing involves the raw data that was collected at one-minute intervals, which was then aggregated into hourly and daily averages to maintain trends and to make analysis easier. Visual methods, such as box plots and statistical techniques, were performed to identify outliers, which are values that are more than three standard deviations from the mean. After analyzing these outliers, inaccurate data, frequently resulting from sensor errors, was then corrected or eliminated. Furthermore, the correlation analysis was carried out to investigate the connections between the particulate matter (PM) and climatic variables, such as temperature and humidity, which revealed important trends and dependencies. These methods made sure the dataset was reliable, consistent, and suitability for thorough study.

## 4. Results and Discussion

### *4.1. Descriptive Analysis of Air Quality Parameters*

This section analyzes air quality indices and particulate matter (PM) levels at three locations. Data from 1 January 2023 to 30 April 2023, with a one-minute interval, was collected from the mine site, the mine GM office (HQ), and the IIT–ISM monitoring sensors. Notably, the mining region exhibits the highest pollution levels, followed by the GM office (HQ), with IIT–ISM showing the least pollution. Mean, median, and standard deviation values are detailed in Tables 2–4. The mean concentrations at both the mine site and the mine GM office (HQ) exceeded the permissible limits set by the National Ambient Air Quality Standards (NAAQS) for $PM_{2.5}$ and $PM_{10}$ [50]. This is attributed to dust emissions from opencast mining activities, including drilling, blasting, and excavation [51]. At the mine site (Table 2), the mean concentrations for $PM_1$, $PM_{2.5}$, and $PM_{10}$ were 129.55 $\mu g/m^3$, 159.11 $\mu g/m^3$, and 180.48 $\mu g/m^3$, respectively, surpassing the NAAQS limits. The mine GM office (HQ) data (Table 3) revealed similar exceedances, with mean concentrations of 109.52 $\mu g/m^3$, 134.75 $\mu g/m^3$, and 153 $\mu g/m^3$ for $PM_1$, $PM_{2.5}$, and $PM_{10}$, respectively. By contrast, the IIT–ISM (Table 4) recorded concentrations below the NAAQS limits, indicating a cleaner environment. The IIT–ISM's mean concentrations for $PM_1$, $PM_{2.5}$, and $PM_{10}$ were 52.55 $\mu g/m^3$, 64.33 $\mu g/m^3$, and 74.6 $\mu g/m^3$, respectively. The mean air quality i8ndex (AQI) values for the mine site, the mine GM office (HQ), and the IIT–ISM were calculated to be 258.47, 234.71, and 123.75, respectively. According to the classification provided by the United States Environmental Protection Agency (US EPA) in 1997, the AQI for the mine site and the mine GM office (HQ) are falls within the 'very unhealthy' category, indicative of heightened health concerns associated with poor air quality. By contrast, the AQI for the IIT–ISM falls under the 'unhealthy for sensitive groups' category, suggesting a relatively better air quality environment at that location during the study period [52]. This classification underscores notable variations in air quality across the monitored locations, reflecting the impact of local factors on atmospheric conditions and the potential health risks for individuals exposed to different levels of air pollution. For a detailed breakdown of AQI values and categories based on Indian standards, please refer to Tables 5 and 6.

The mean $PM_{10}$ concentration at the mine site is 1.8 times higher than the National Ambient Air Quality Standards (NAAQS) permissible limit of 100 $\mu g/m^3$, while at the mine GM office (HQ), it is 1.53 times higher. Similarly, the mean $PM_{2.5}$ concentration at the mine site is 2.65 times higher than the NAAQS limit of 60 $\mu g/m^3$, and 2.24 times higher at the mine GM office (HQ). The elevated PM levels at the mine site, located approximately 200 m from the mine boundary, are primarily attributed to blasting, coal and overburden (OB) loading and transportation, and the movement of heavy earth-moving machinery (HEMM). The mine GM office (HQ), situated 1.5 km from the mine boundary, also experiences high PM concentrations due to operations in a nearby mine site in Jharkhand. However, the

mean concentrations of $PM_1$, $PM_{2.5}$, and $PM_{10}$ at the mine GM office (HQ) are slightly lower than those at the mine site due to its location in a residential area surrounded by buildings and vegetation that mitigate pollution levels. By contrast, the IIT–ISM, located 12 km from the mine, records satisfactory PM concentrations, as its distance from mining activities and dense vegetation significantly reduce pollutant levels compared to the mine site and the mine GM office (HQ).

**Table 2.** Data analysis of measured values of PM and AQI at the mine site (industrial zone).

| | $PM_1$ | $PM_{2.5}$ | $PM_{10}$ | Temp (Cel.) | Hum | AQI-IN |
|---|---|---|---|---|---|---|
| Count | 172,800 | 172,800 | 172,800 | 172,800 | 172,800 | 172,800 |
| Mean | 129.55 | 159.11 | 180.48 | 23.81 | 59.68 | 258.97 |
| SD | 75.07 | 91.14 | 103.22 | 5.25 | 11.75 | 113 |
| Min. | 26.81 | 33.46 | 37.54 | 12.27 | 30 | 56.35 |
| 25% | 72.54 | 88.82 | 101.64 | 19.65 | 50.84 | 172.98 |
| 50% | 110.33 | 136.12 | 154.29 | 23.92 | 60.42 | 244.65 |
| 75% | 165.68 | 203.38 | 230.8 | 27.55 | 69.31 | 311.49 |
| Max. | 358.82 | 437.99 | 496.27 | 34.97 | 83.08 | 575.38 |

**Table 3.** Descriptive statistics for the mine GM office (HQ) (Buffer Zone).

| | $PM_1$ | $PM_{2.5}$ | $PM_{10}$ | Temp (Cel.) | Hum | AQI-IN |
|---|---|---|---|---|---|---|
| Count | 172,800 | 172,800 | 172,800 | 172,800 | 172,800 | 172,800 |
| Mean | 109.52 | 134.75 | 153.0 | 24.81 | 54.76 | 234.71 |
| SD | 63.37 | 77.34 | 88.24 | 5024 | 14.3 | 101.56 |
| Min. | 30.65 | 38.21 | 43.4 | 11.35 | 23.39 | 67.63 |
| 25% | 67.73 | 83.5 | 94.79 | 21.39 | 43.09 | 166.08 |
| 50% | 89.29 | 109.88 | 125.86 | 25.17 | 55.02 | 208.42 |
| 75% | 120.59 | 148.22 | 169.21 | 28.46 | 64.16 | 275.12 |
| Max. | 355.85 | 436.14 | 496.98 | 34.83 | 84.71 | 563.62 |

**Table 4.** Descriptive Statistics for IIT–ISM (Sensitive Zone).

| | $PM_1$ | $PM_{2.5}$ | $PM_{10}$ | Temp (Cel.) | Hum | AQI-IN |
|---|---|---|---|---|---|---|
| Count | 172,800 | 172,800 | 172,800 | 172,800 | 172,800 | 172,800 |
| Mean | 52.55 | 64.33 | 74.6 | 26.5 | 44.3 | 123.75 |
| SD | 16.57 | 22.43 | 26.18 | 5.2 | 12.54 | 47.53 |
| Min. | 23.02 | 28.42 | 32.21 | 17.21 | 22.04 | 47.79 |
| 25% | 40.93 | 45.39 | 54.68 | 22.17 | 32.6 | 85.63 |
| 50% | 49.62 | 62.34 | 70.07 | 27.01 | 43.93 | 114.29 |
| 75% | 64.05 | 78.66 | 92.91 | 30.61 | 54.98 | 154.32 |
| Max. | 93.57 | 138.05 | 146.2 | 36.48 | 71.41 | 256.01 |

**Table 5.** AQI category based on Indian standards.

| AQI Value | AQI Category | AQI Color |
|---|---|---|
| 0–50 | Good | Green |
| 51–100 | Moderate | Yellow |
| 101–150 | Unhealthy for sensitive groups | Orange |
| 151–200 | Unhealthy | Red |
| 201–300 | Very unhealthy | Purple |
| 300–500 | Hazardous | Maroon |

**Table 6.** Air quality standards of different organizations.

| Pollutants | Period of Collection | Coal Mines Regulation Act (CMRA) 2017 | India (NAAQS) | (WHO 2021) AQGs | No of Times Threshold Limit Exceeded at Mine Site Mine Based on CMRA |
|---|---|---|---|---|---|
| $PM_{2.5}$ ($\mu g/m^3$) | Annual | 215 | 40 | 5 | 23 |
| | 24-hr | 300 | 60 | 15 | |
| $PM_{10}$ ($\mu g/m^3$) | Annual | 215 | 40 | 5 | 21 |
| | 24-hr | 300 | 60 | 15 | |
| $O_3$ ($\mu g/m^3$) | Peak Season | 100 | 100 | 60 | 40 |
| | 8-hr | 180 | 180 | 100 | |
| $NO_2$ ($\mu g/m^3$) | Annual | 80 | 40 | 10 | 51 |
| | 24-hr | 120 | 80 | 25 | |
| $SO_2$ ($\mu g/m^3$) | Annual | 80 | 50 | 60 | 34 |
| | 24-hr | 120 | 80 | 40 | |
| CO ($\mu g/m^3$) | 24-hr | 4 | 4 | 4 | 18 |

### *4.2. Box Plots and Probability Density Plots*

An analysis of the box plots depicting $PM_1$, $PM_{2.5}$, $PM_{10}$, and AQI values for over the three separate monitoring stations gives interesting results about air quality patterns (Figure 7). These data highlight not only the spread of pollutants but the disparities between the mine site, the mine GM office (HQ), and the IIT–ISM. The boxes indicating $PM_1$, $PM_{2.5}$, $PM_{10}$, and AQI at the mine site appear widely spread. The boxes for similar metrics at the IIT–ISM, on the other hand, are noticeably less spread out, suggesting more consistent air quality. However, it is essential to highlight that the mine GM office (HQ) regularly has the highest number of outliers, indicating more fluctuation in air quality data. Furthermore, at the mine GM office (HQ), all four parameters ($PM_1$, $PM2_{2.5}$, $PM_{10}$, and AQI) have the highest positive skewness, indicating that much of the data is concentrated on the left side, representing smaller values. By contrast, the data distribution at the IIT–ISM is more symmetrical, with less apparent skewness. Explicitly focusing on the $PM_1$ data, the median line for the IIT–ISM falls below the boxes for the mine site and the mine GM office (HQ), indicating likely differences in $PM_1$ levels between these locations. Similar patterns emerge in the box plots for the $PM_{2.5}$ and $PM_{10}$ data. Our findings highlight a strong correlation between $PM_{2.5}$, $PM_{10}$, and $PM_1$, emphasizing the interconnected nature of different particulate sizes. Fine particles ($PM_1$ and $PM_{2.5}$) are primarily produced by combustion processes and secondary reactions in the atmosphere, while coarser particles ($PM_{10}$) are typically generated by mechanical activities, like mining and construction. Fine particles are often present within the larger $PM_{10}$ fraction, leading to a high correlation between these categories. Moreover, we have identified production activities as a significant contribution to PM, stressing the need for effective mitigation strategies within the mining sector. Furthermore, our differentiation of monitoring sites, encompassing actual mines, residential areas, offices, and university campuses, provides a nuanced perspective on air quality variations in diverse settings.

The box plot in Figure 8 represents the cumulative particle counts for three size ranges: particle count (1.0) for sizes 1 µm and above, particle count (0.5) for sizes 0.5 µm and above (including 1 µm and above), and particle count (0.3) for sizes 0.3 µm and above (including 0.5 µm and 1 µm and above). This cumulative approach provides a comprehensive view of particle distribution, where larger particles are naturally fewer in number, and smaller particles dominate the overall count.

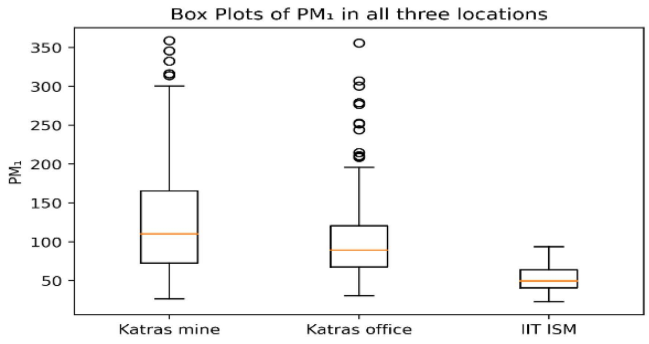


Box Plot of $PM_1$

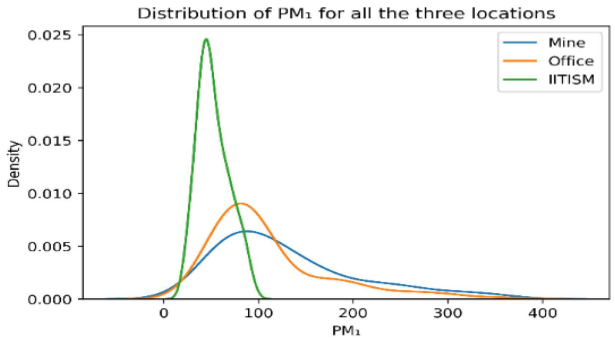


Distribution of $PM_1$

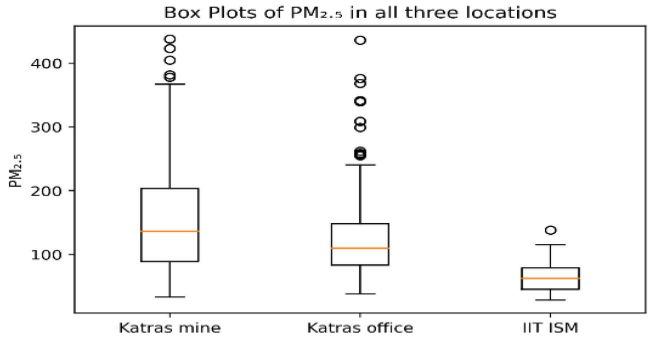


Box Plot of $PM_{2.5}$

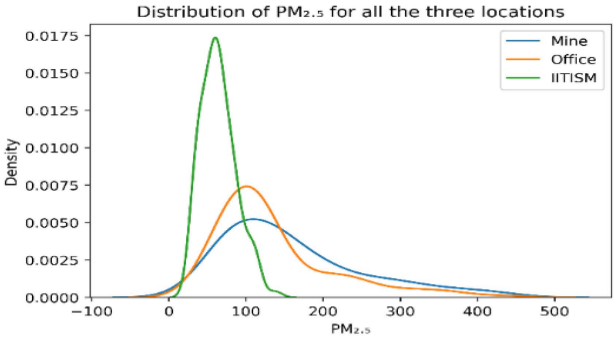


Distribution of $PM_{2.5}$

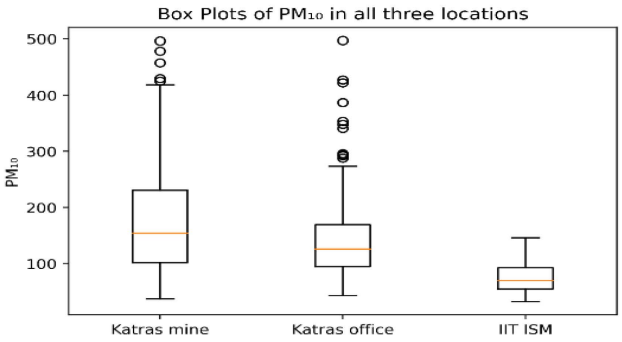


Box Plot of $PM_{10}$

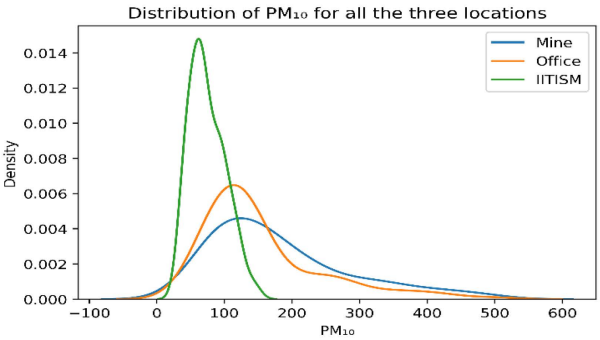


Distribution of $PM_{10}$

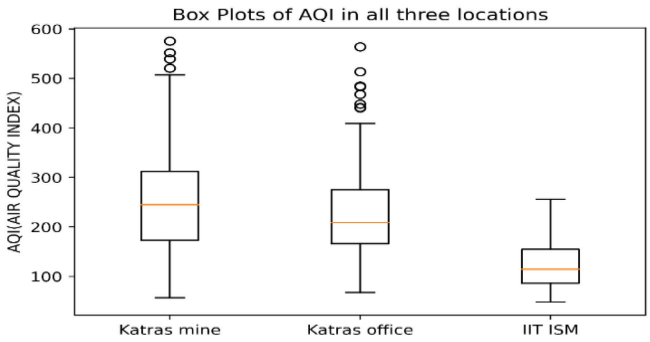


Box Plot for AQI

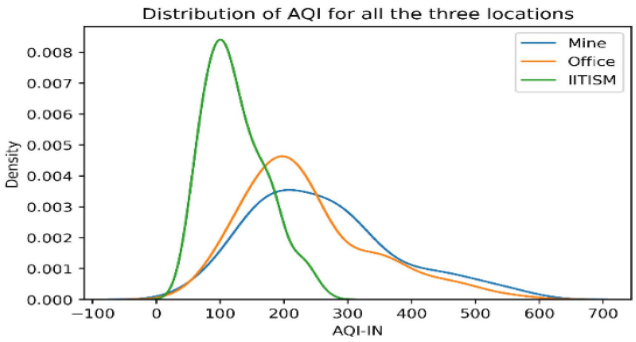


Distribution for AQI

**Figure 7.** Box Plot and Distribution Plots Visualizations for PMs and AQI.

The decision to use cumulative particle counts is based on several key factors. First, this approach reflects the real-world distribution of airborne particulate matter, capturing particles across a range of sizes and ensuring that all particles larger than a specific threshold

are accounted for. Second, it aligns with the hierarchical inclusion of particle sizes, where smaller size ranges inherently encompass larger particles, mirroring the nested structure of particulate matter. Additionally, the relative contribution of smaller particles to the total count can be clearly compared across size ranges by cumulative grouping. This method also streamlines data analysis while offering significant insights into the abundance of both small and large particles by eliminating the complexity of size categories that are mutually exclusive. Additionally, it is also relevant to the environment and human health because smaller particles, such as those smaller than 0.3 μm, are particularly dangerous because of their capacity to enter lungs easily. Cumulative counts are useful for examining the effects on the environment and human health because they allow for a more accurate assessment of the overall burden of particles in each size range.

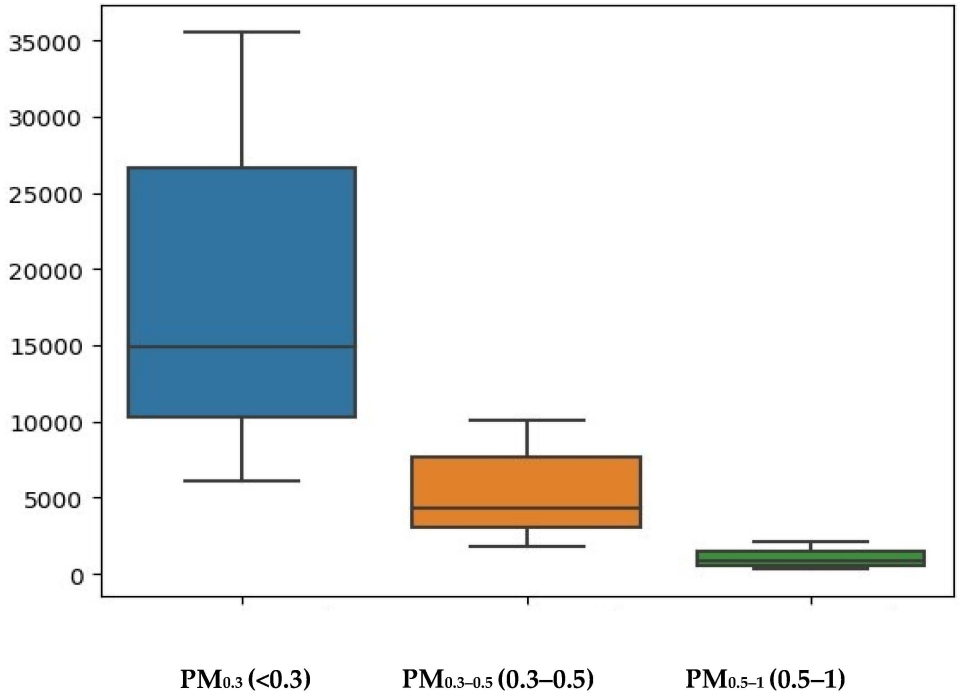


**Figure 8.** Distribution of Particle Counts Across Different Size Ranges.

In the box plot, particle count (1.0) shows the smallest cumulative count, clustering around 2500, as it includes only particles ≥1 μm, which are less abundant. Particle count (0.5) is higher, approximately 7500, as it includes particles ≥ 0.5 μm (including those ≥ 1 μm). Finally, particle count (0.3) is the highest, with an interquartile range (IQR) of 10,000 to 25,000 and a median of 15,000, reflecting its inclusion of all particles ≥ 0.3 μm. This cumulative approach effectively highlights the abundance and variability of particles across different size ranges, providing a clear and logical understanding of their distribution.

### *4.3. Spatiotemporal Variations in PM Levels*

This section presents the analysis of line plots for $PM_1$, $PM_{2.5}$, and $PM_{10}$ measured at the mine site, the mine GM office (HQ), and the IIT–ISM over four months, from 1 January 2023 to 30 April 2023. Across all three monitoring sites, PM concentration reached its highest level in January and remained relatively elevated from February to April, largely attributable to the extensive mining activities. This connection can be established by examining coal production data for these months (Figure 9). The total excavated material is the sum of coal production plus the overburden removed to get to the coal. The line graphs depicting the relationship between total excavation and months reveal a meaningful

connection: January's total production was the highest among the four months. This implies that coal production and associated activities significantly contribute to elevated PM concentrations. Similarly, February's PM concentration was lower than January's but higher than March's and April's. This again reinforces the observation that coal production and associated operational activities were higher than in March and April but lower than in January (Table 1). The high PM concentration is attributed to coal and OB blasting, coal and OB loading, transportation, and heavy earth-moving machinery movement [53]. The mean $PM_{2.5}$ level at the mine site is 2.65 times higher than the permissible limit of 60 at industrial sites. It is observed that, during the months of January and February, the $PM_{2.5}$ concentrations exceeded the threshold limits the most. The threshold value was exceeded less often during March and April than in the previous two months. Figure 10 shows the plots of $PM_1$, $PM_{2.5}$, and $PM_{10}$ concentrations at the mine site monitoring on a particular day of each of the four months from January to April, respectively.

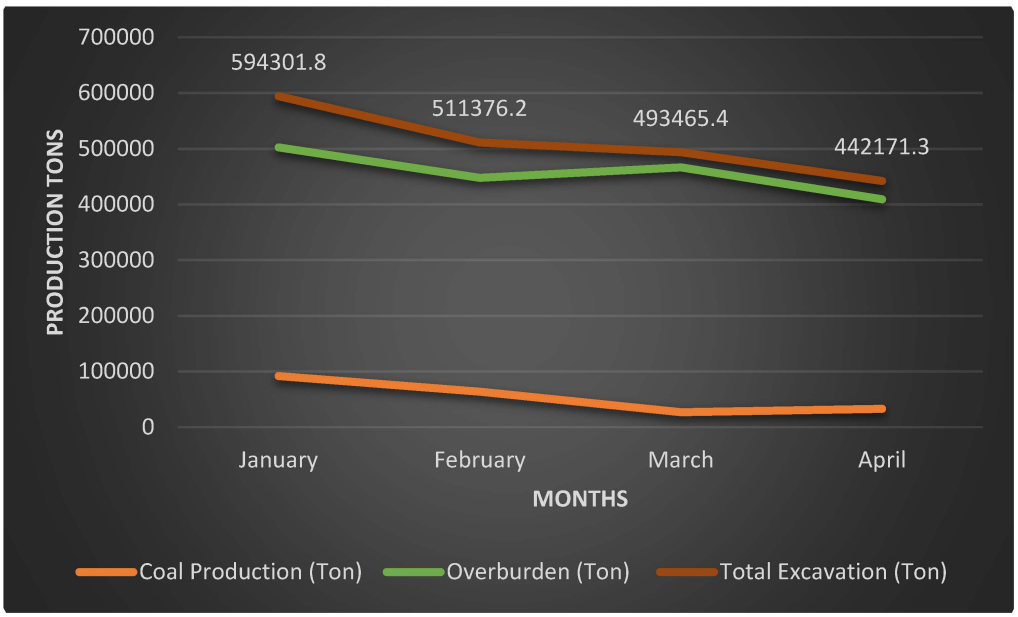


**Figure 9.** Total excavation in respective months from January to April.

### *4.4. Diurnal Variations in PM Concentrations and Meteorological Influences on PM Concentrations*

The hour-wise plot of PM over a period of 24 h averaging over 30 days of the month for all four months can be seen in Figure 11 for the mine site monitoring station data. Two peaks are clearly visible; one is during the morning around 6:00 a.m., and the other lower peak in concentration is around 6.00 p.m. daily. These peaks align with the lowest temperatures of the day, demonstrating the influence of temperature inversions. During cooler early mornings, temperature inversions trap PM near the ground, preventing vertical dispersion and causing peak concentrations. This effect is depicted in Figure 11**,** where PM concentrations peak around 6:00 a.m. daily. For instance, the mean $PM_{2.5}$ level at the mine site during this period exceeded 159 $\mu g/m^3$, which is 2.65 times the National Ambient Air Quality Standards (NAAQS) limit of 60 $\mu g/m^3$, and $PM_{10}$ concentrations reached 180 $\mu g/m^3$, 1.8 times the permissible limit of 100 $\mu g/m^3$. Conversely, rising daytime temperatures promote atmospheric mixing and pollutant dispersion, leading to lower PM levels, as evident from the negative correlation between temperature and PM, with an $R^2$ value of 0.45 at the mine site (Figures 12 and 13).

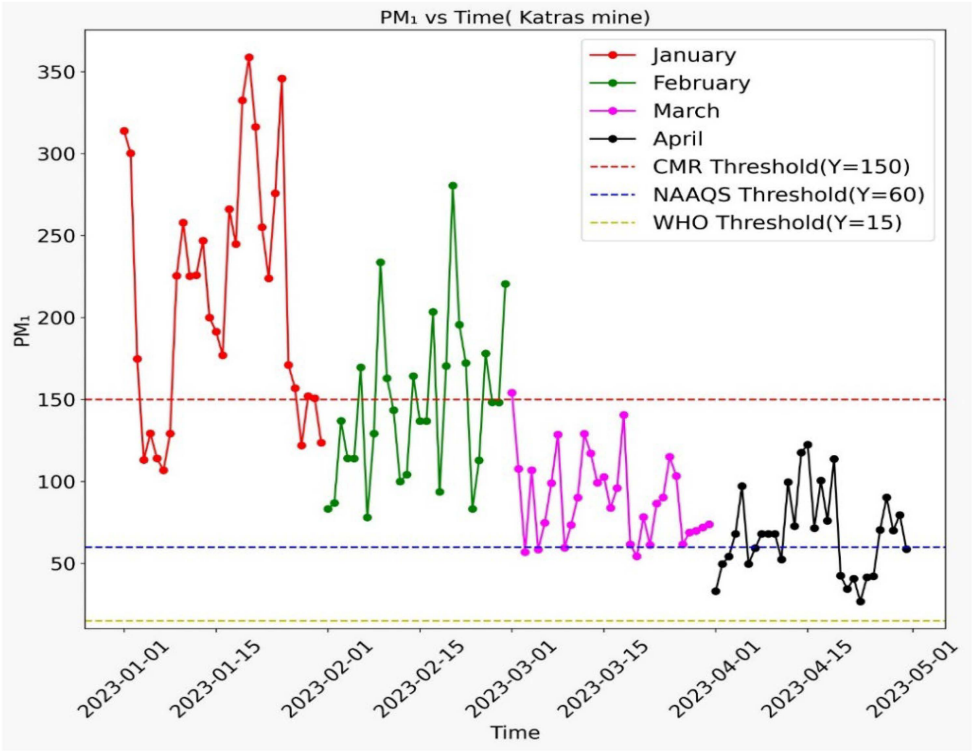


(**a**)

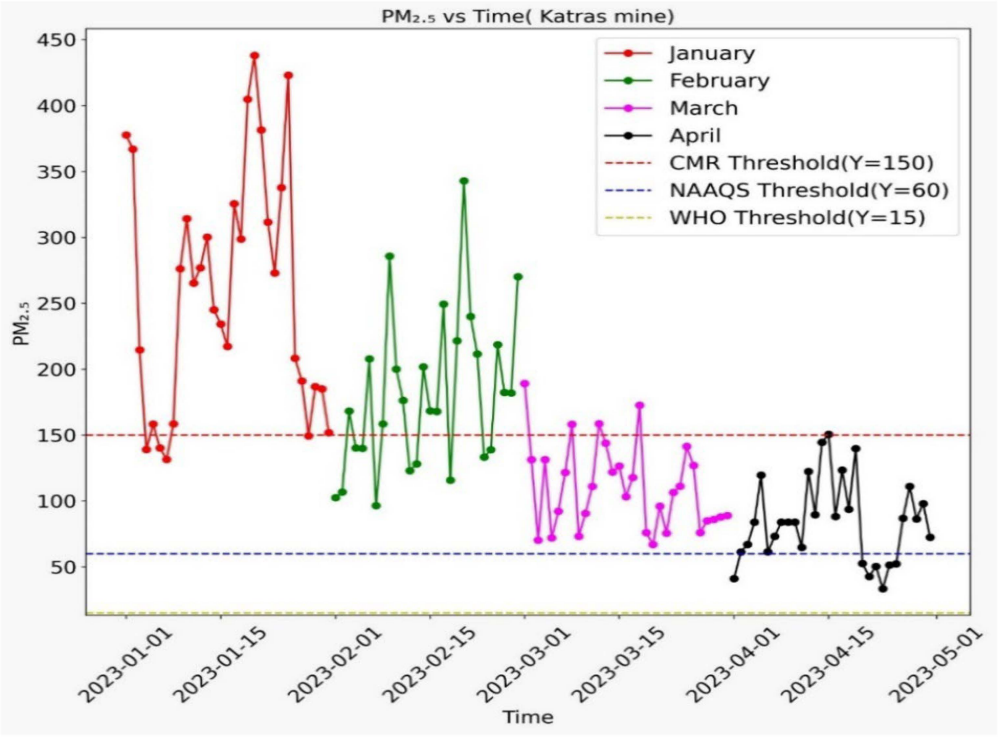


(**b**)

**Figure 10.** *Cont*.

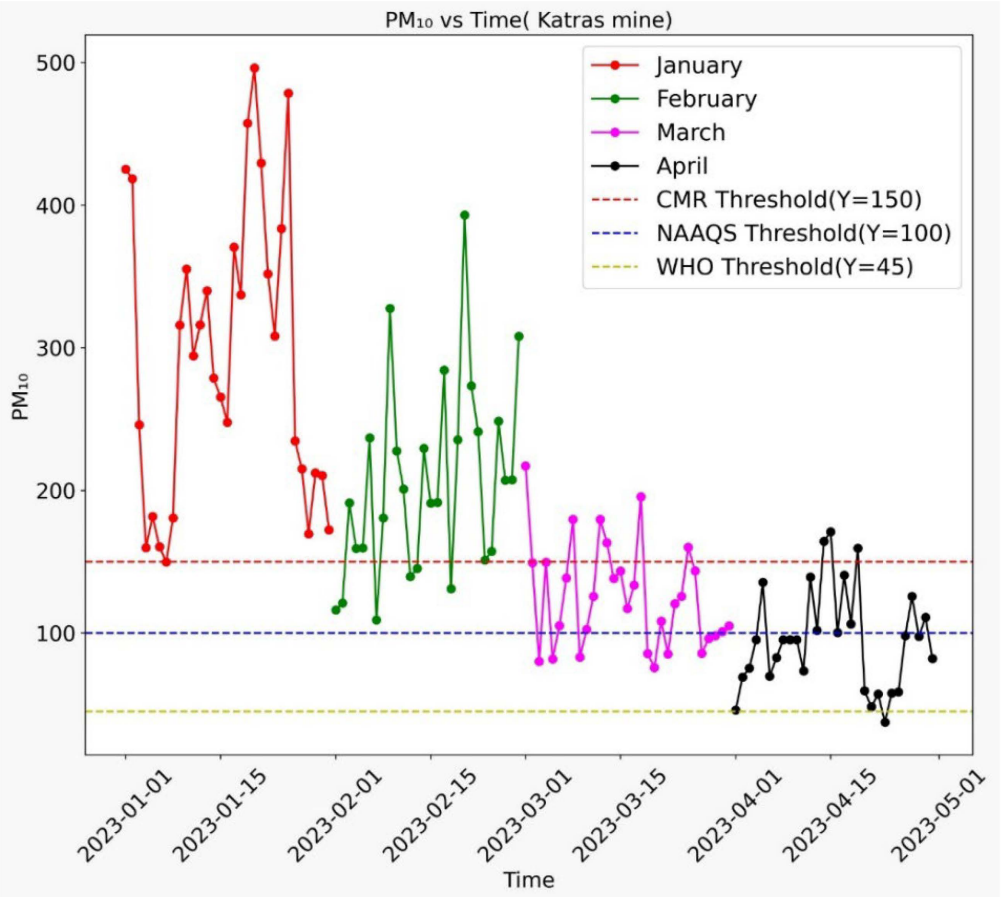


(**c**)

**Figure 10.** Daily average peaks of PM concentration at the mine site from January to April 2023. (**a**) Daily average of $PM_1$ at the mine site from January to April 2023. (**b**) Daily average of $PM_{2.5}$ at the mine site from January to April 2023. (**c**) Daily average of $PM_{10}$ at the mine site from January to April 2023.

As temperature decreases in the early morning, humidity simultaneously increases, with relative humidity levels exceeding 70% (Figure 14). This elevated humidity enhances the growth of hygroscopic particles, further contributing to PM accumulation. As shown in Figure 14, the relationship between humidity and PM concentrations is particularly evident, with elevated humidity levels contributing to PM accumulation by absorbing solar radiation and weakening vertical air currents. For instance, $PM_{10}$ concentrations at the mine site exceeded 180 $\mu g/m^3$ during high humidity periods, 1.8 times the permissible limit of 100 $\mu g/m^3$. Scatterplots in Figures 12 and 13 further demonstrate a positive correlation between humidity and PM levels, supported by second-degree polynomial curves fitted to all relationships at the mine Site for $PM_1$, $PM_{2.5}$, and $PM_{10}$. These trends underscore how high humidity exacerbates PM accumulation, while higher daytime temperatures improve dispersion, and the combined effects of temperature and humidity, as demonstrated in the study's visualizations, which provide critical insights into PM dynamics in mining regions.

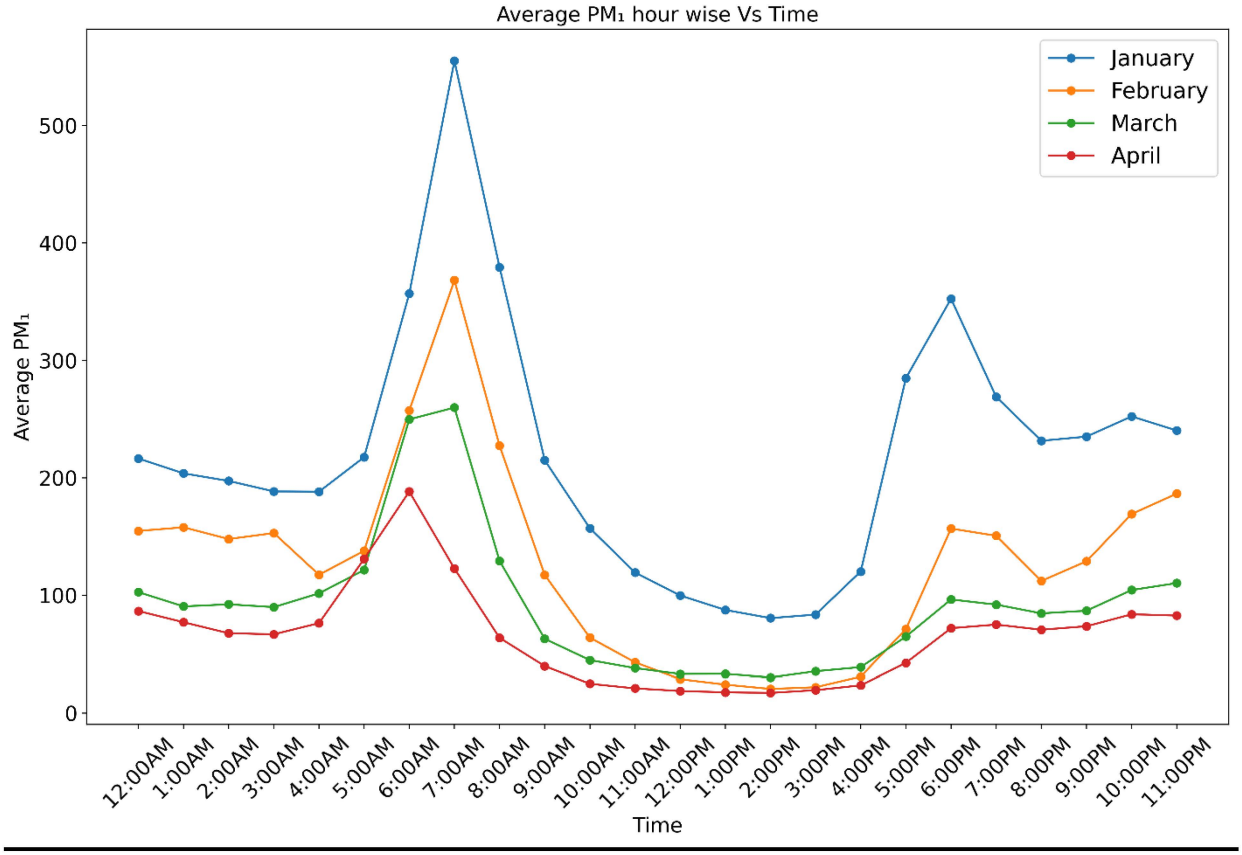


(**a**)

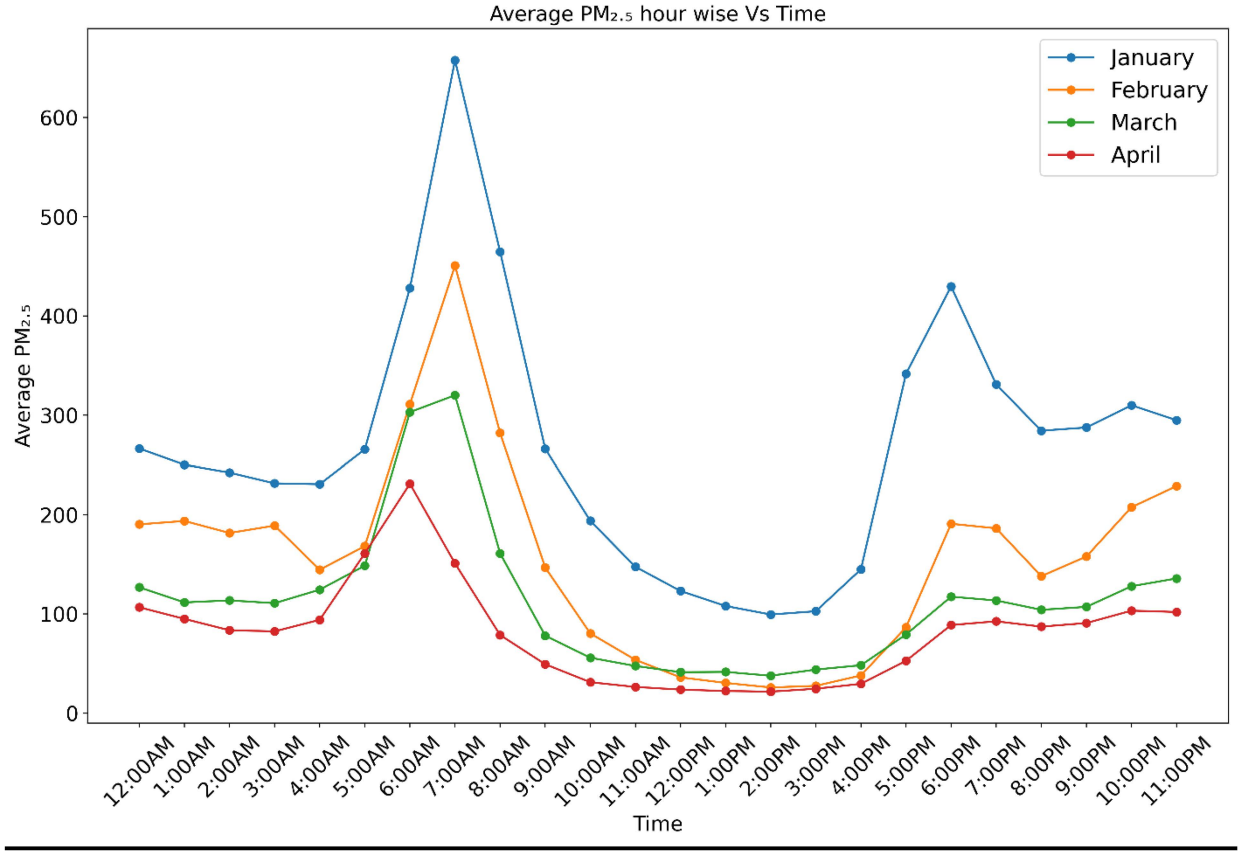


(**b**)

**Figure 11.** *Cont.*

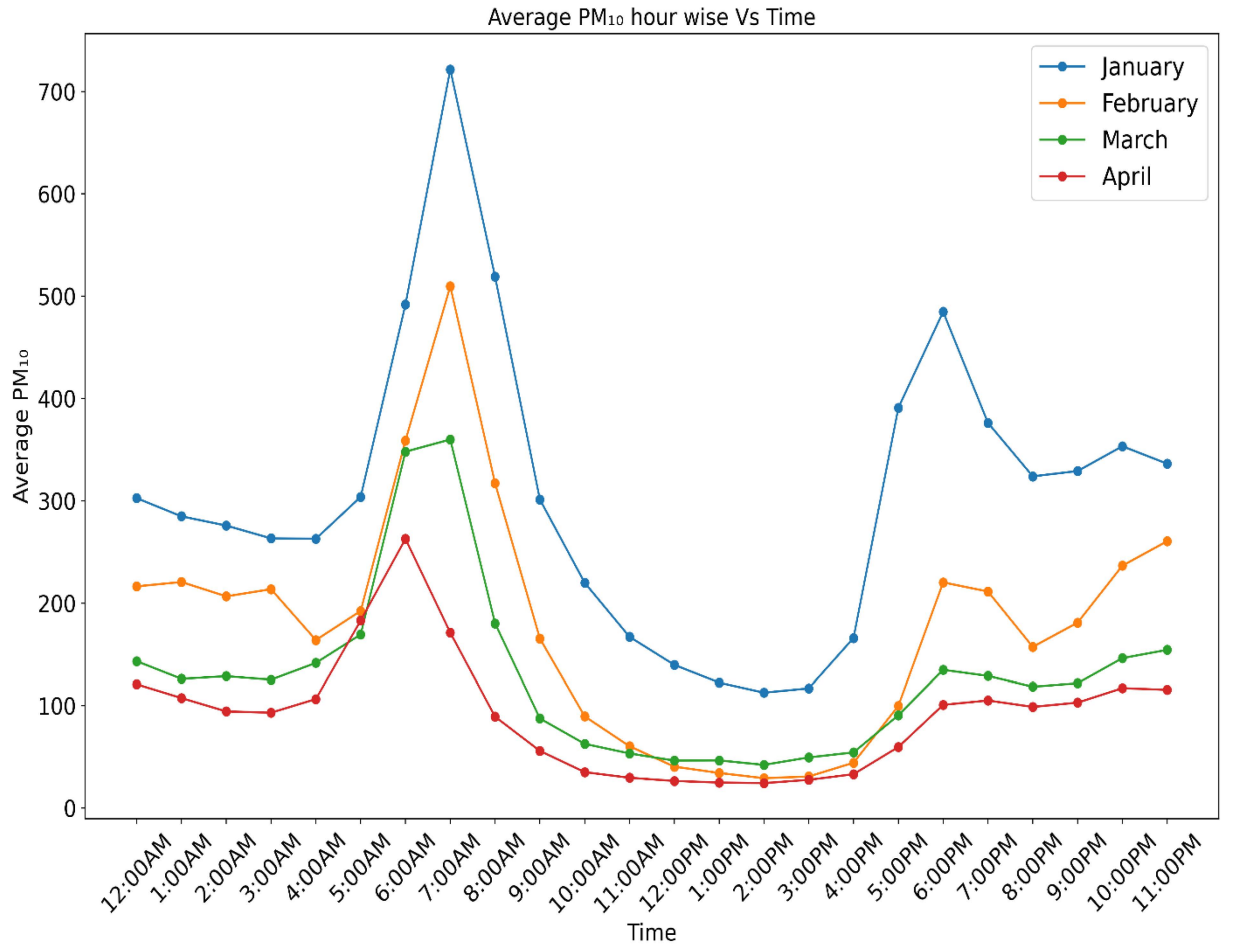


(**c**)

**Figure 11.** Hourly average concentration of PM vs. Time. (**a**) Average concentration of $PM_1$ Vs. Hour. (**b**) Average $PM_{2.5}$ Hour wise vs. Time. (**c**) Average concentration of $PM_{10}$ vs. Hours.

$PM_1$ concentrations at the opencast coal mine exhibit substantial fluctuations during peak transportation operating hours, displaying a clear upward trend before reaching peak levels. This observation strongly indicates that transportation activities substantially impact rising $PM_1$ concentrations [54]. Lastly, a peak at around 6:00 p.m., which can be observed in Figure 11, is due to blasting operations, which are planned to occur between 3:00 p.m. and 6:00 p.m. every day, and concurrent shift change activities, such as the movement of HEMM and workers arrival and departure [13,26,55]. These results highlight the relation between multiple factors that influence the peak PM concentrations in the mine. Understanding these dynamics is crucial for developing effective mitigating and managing strategies for particulate matter pollution in mining operations, particularly during blasting and transportation activities. The overall air quality measure has a similar trend, as shown in Figure 15.

By contrast, data from the IIT–ISM (Figure 16) reveal a different pattern. Scatterplots of $PM_{2.5}$ against temperature and humidity at this site show randomly distributed points, with no discernible trends or correlations. Unlike the mine site, where meteorological factors significantly influence PM levels, the absence of a second-degree curve in Figure 16 indicates very weak or no correlation between $PM_{2.5}$ and temperature or humidity at the IIT–ISM. This lack of correlation can be attributed to the IIT–ISM's distance from mining activities and its dense vegetation cover, which mitigates PM concentrations and minimizes the impact of temperature and humidity on air quality.

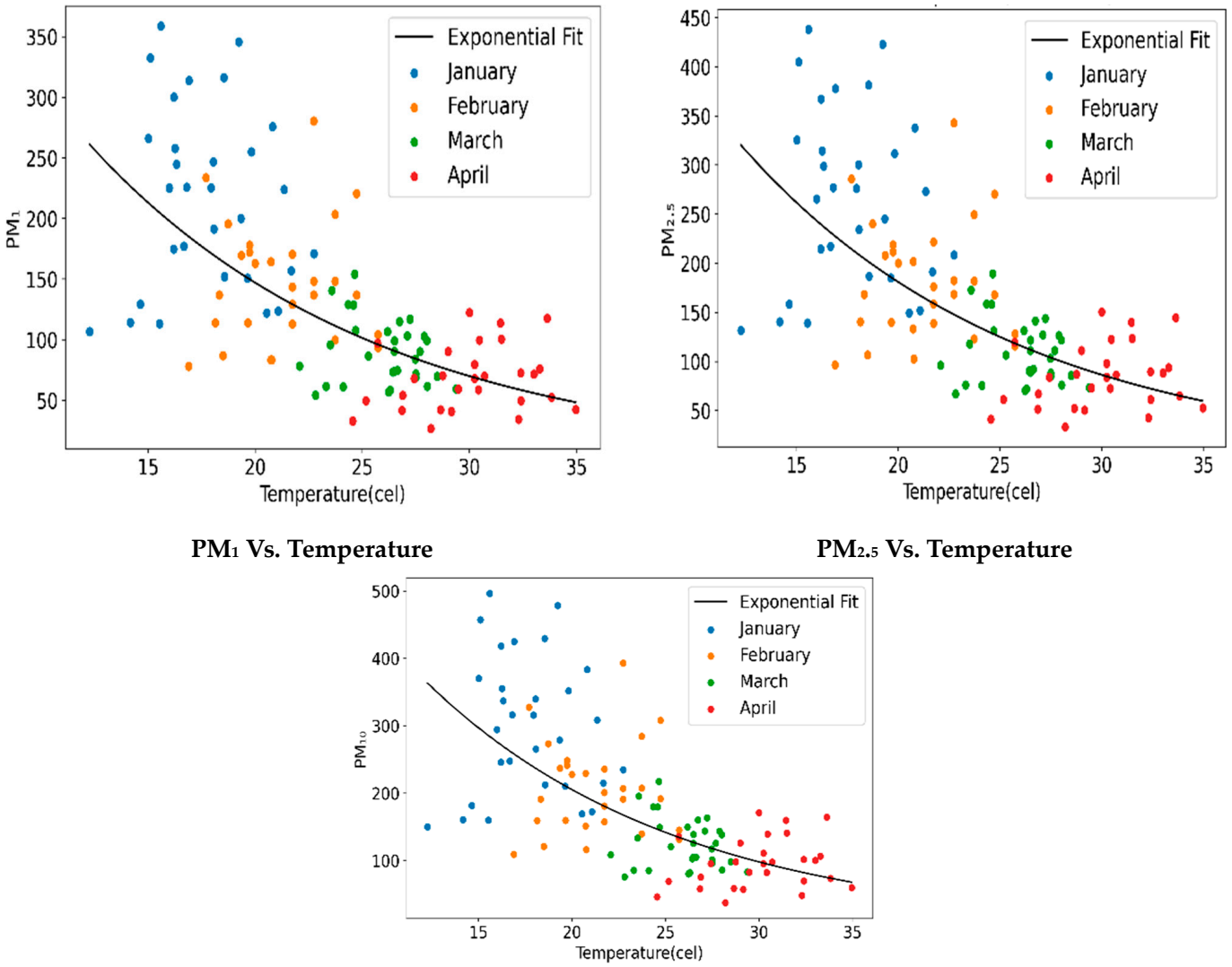


**Figure 12.** Fitting a second-degree curve to the scatterplots of $PM_1$, $PM_{2.5}$, and $PM_{10}$ vs. temperature at the mine site.

These findings highlight the localized nature of meteorological influences on PM concentrations. At the mine site, temperature inversions and high humidity strongly affect PM levels, as seen in Figures 12 and 13. However, at the IIT–ISM, these effects are negligible due to its favorable location and environmental conditions, as depicted in Figure 16. This variation underscores the importance of site-specific strategies to address air quality challenges effectively.

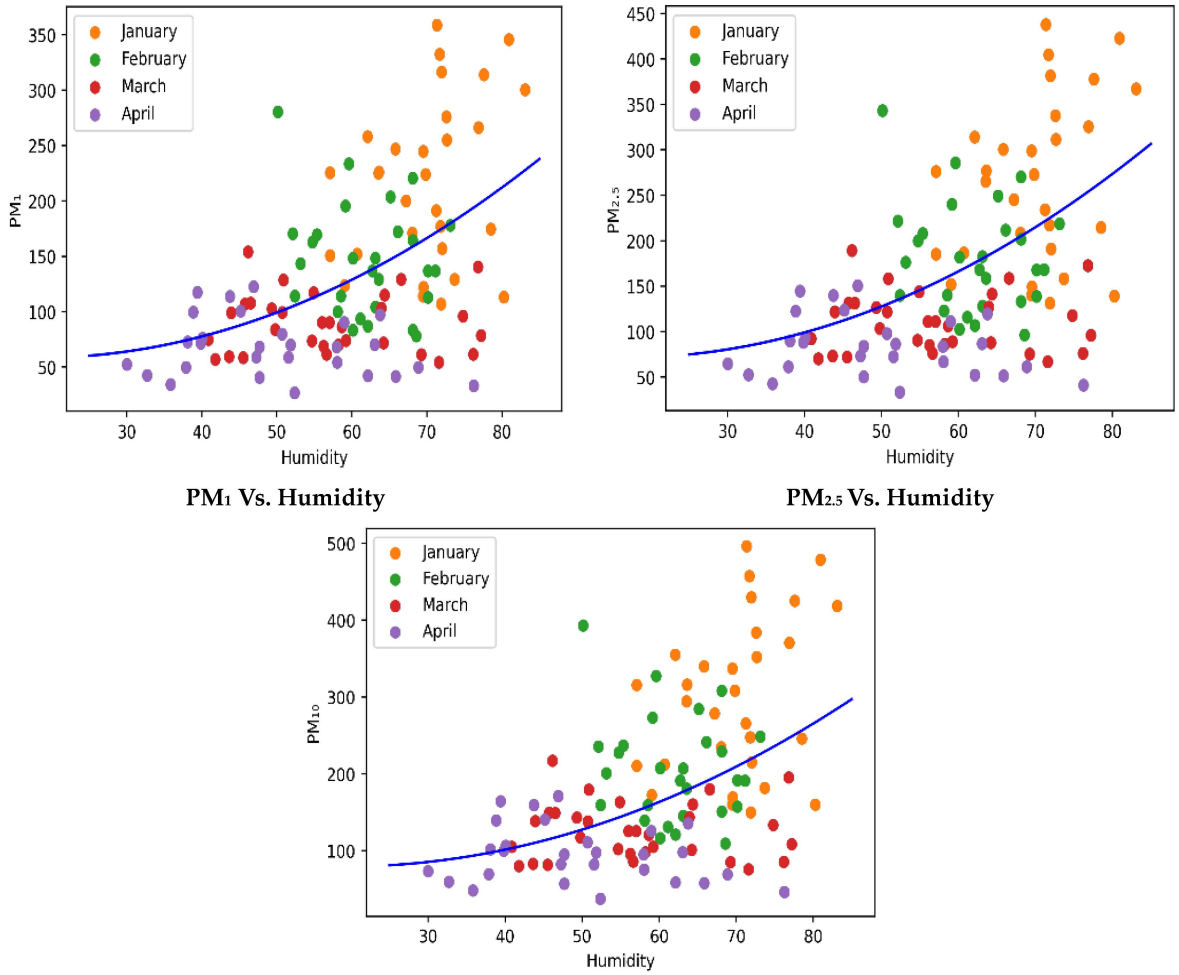


**PM1 Vs. Humidity** **PM2.5 Vs. Humidity**

**PM10 Vs. Humidity**

**Figure 13.** Fitting a second-degree curve to the scatterplots of $PM_1$, $PM_{2.5}$, and $PM_{10}$ vs. humidity at the mine site.

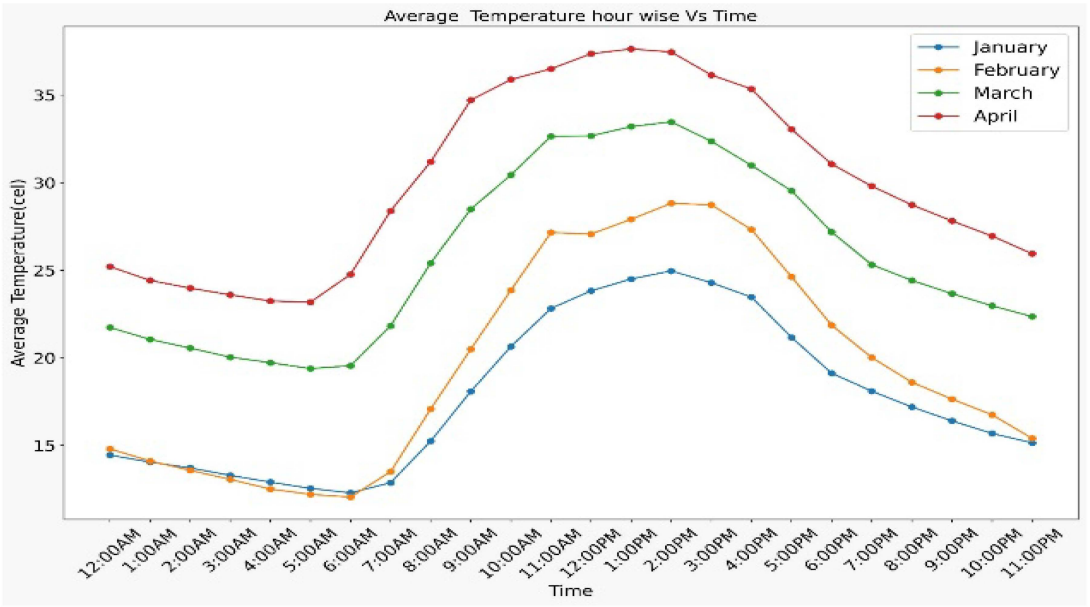


(**a**)

**Figure 14.** *Cont.*

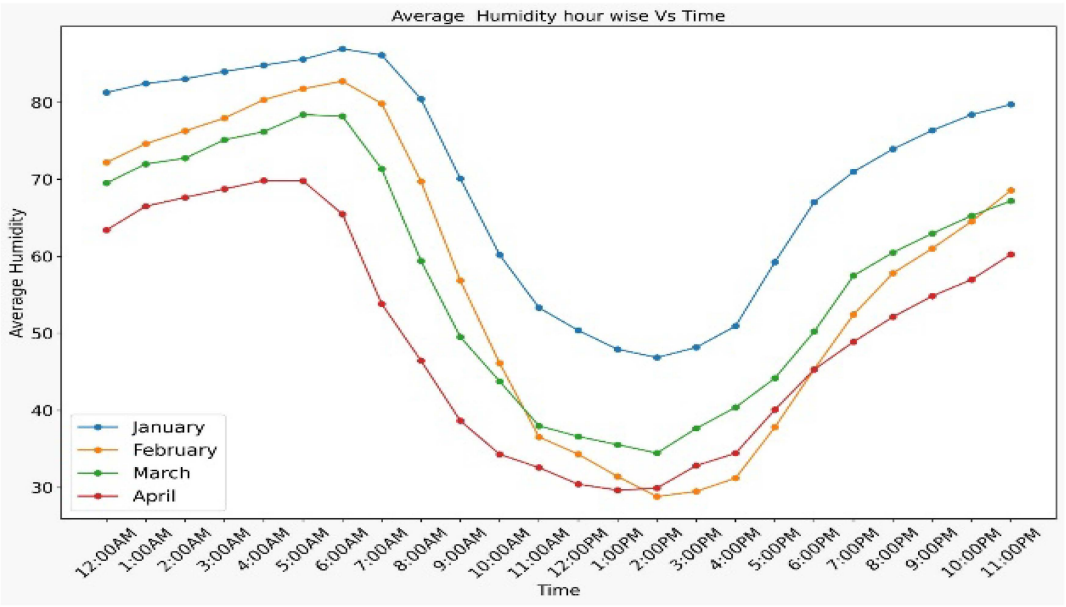


(**b**)

**Figure 14.** Hourly average temperature and humidity of the mine site. (**a**) Hourly average temperature. (**b**) Hourly average humidity.

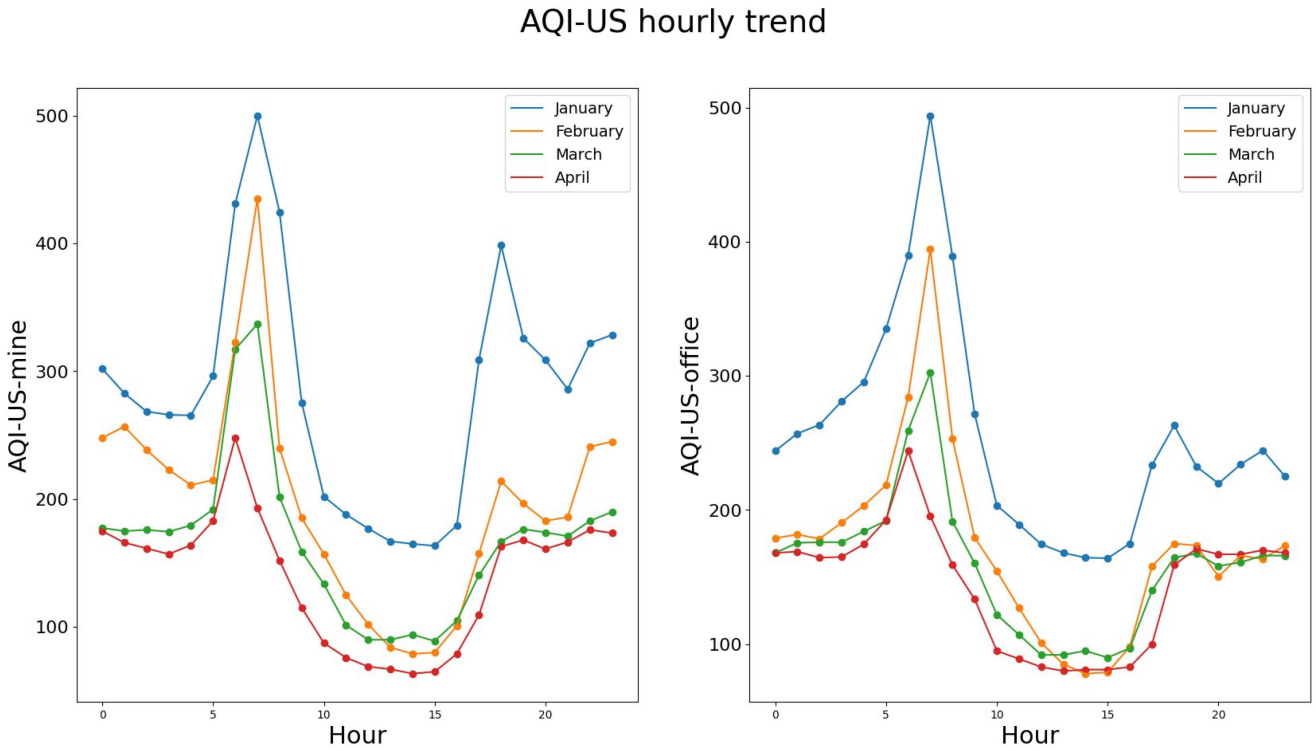


**Figure 15.** Hourly peaks of AQI in the mine site vs. the mine GM office (HQ).

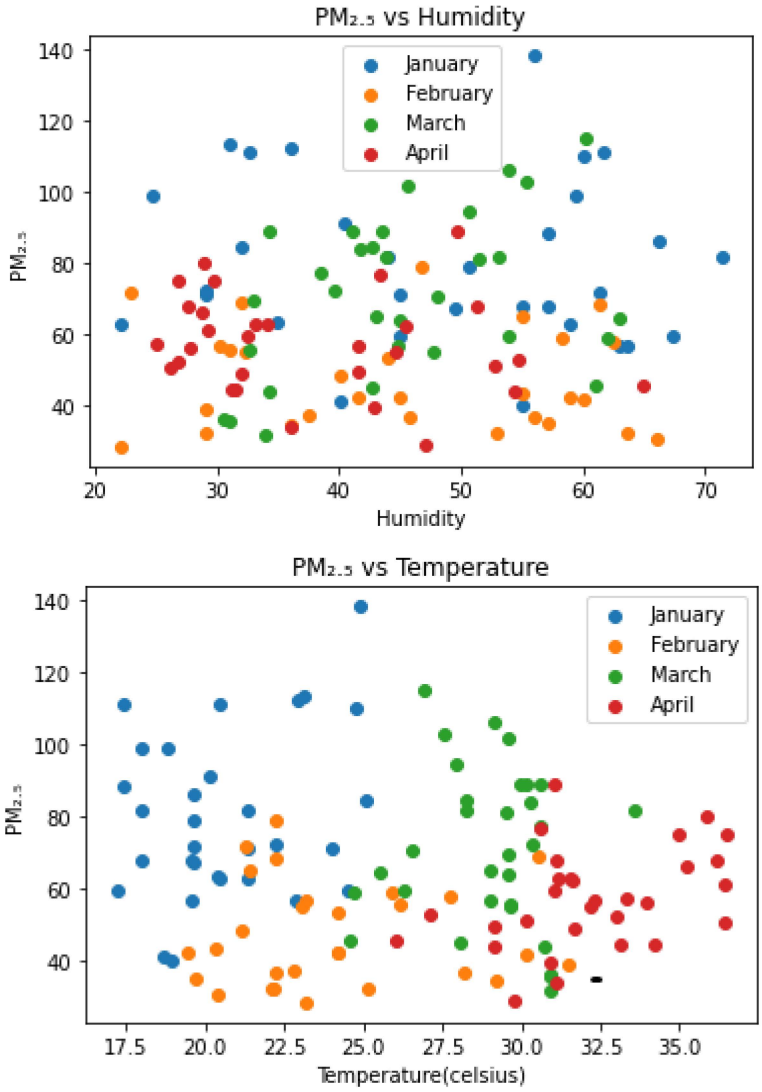


**Figure 16.** Humidity and temperature vs. $PM_{2.5}$ (IIT–ISM).

### *4.5. $PM_{2.5}/PM_{10}$ Ratio and Particle Size Distribution*

The $PM_{2.5}/PM_{10}$ ratio analysis reveals various important insights, as presented in Figure 17. The average $PM_{2.5}/PM_{10}$ ratio is higher than 0.8 at all three locations. A high $PM_{2.5}/PM_{10}$ ratio usually indicates that fine particles and secondary particulates, such as $NO_3$, $SO_4^{2-}$, $NH_4$, and other organic compounds, are the major contributors to the monitoring data set. On the other hand, a lower ratio indicates that coarse particles predominate. This further suggests that the leading causes of PM are these coarse particles produced by natural processes, such as soil erosion, fugitive sand or coal dust, and the long-range transport of sand or coal dust. The average $PM_{2.5}/PM_{10}$ ratio at the mine site, the mine office (HQ), and the IIT–ISM for the study were 0.882 (88.2%), 0.88 (88%), and 0.86 (86%), respectively, which signifies slightly elevated levels of $PM_{2.5}$ than coarse $PM_{10}$ particles. $PM_{2.5}$ can arise from various sources, including seasonality [56], mining operations, and the combustion of fuels. Additionally, it can be formed through reactions involving NOx and SOx with oxidants, such as OH radicals, ozone, etc., leading to the generation of secondary particulates like nitrate and sulfate aerosols [57]. The high ratio at the mine site (0.882 or 88.2%) suggests a significant presence of fine particulate matter ($PM_{2.5}$) relative to coarse particulate matter ($PM_{10}$).

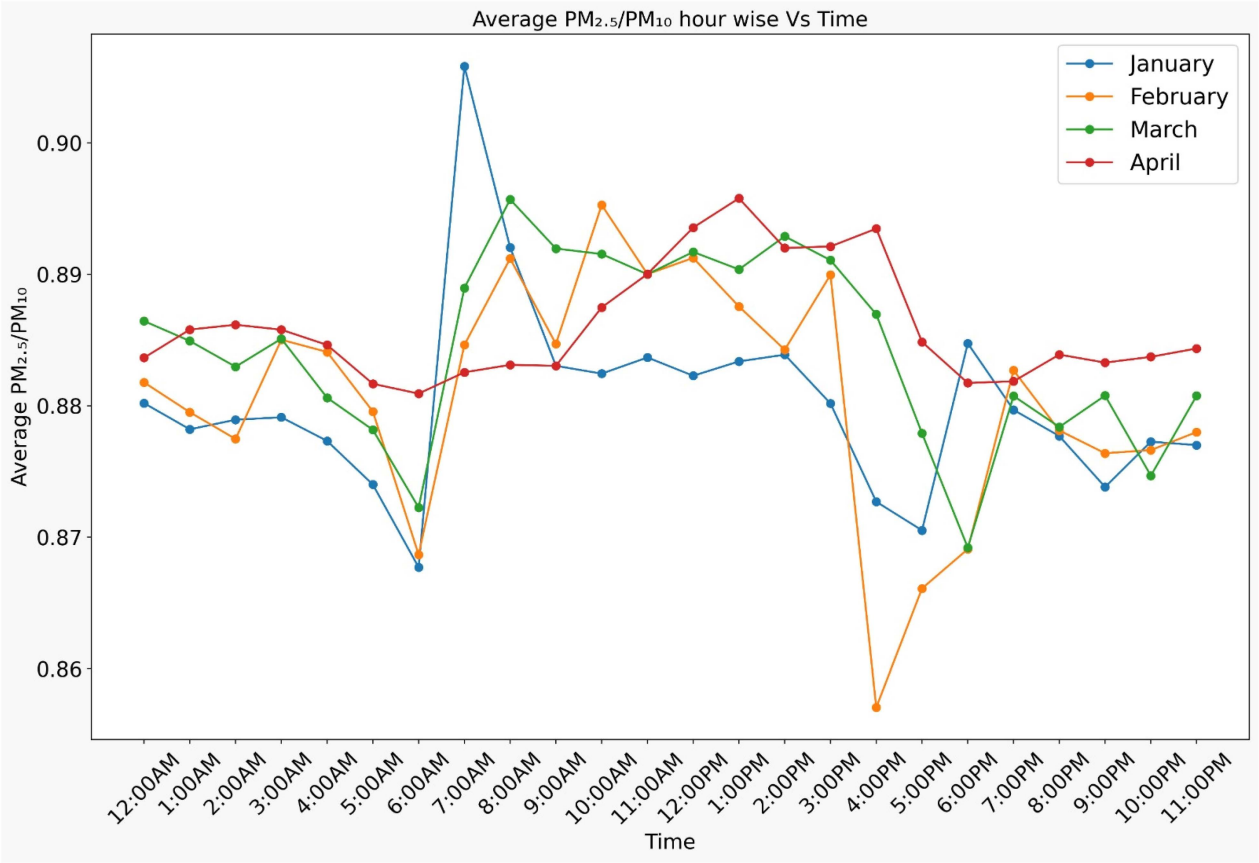


**Figure 17.** $PM_{2.5}/PM_{10}$ ratio at the mine site.

From Figure 17, it can be observed that the $PM_{2.5}/PM_{10}$ ratio is higher during the day, which highlights the effect of temperature on the suspension and movement of fine particles which can easily be carried out by air. The dispersion of coarser particles is prevented by temperature inversions, therefore coarser particles accumulate during early mornings and evenings. These findings suggest that elevated daylight temperatures increase the proportion of fine particulate matter in the air, which poses a greater health risk due to its ability to penetrate deep into the lungs. Therefore, the temperature-driven variations in the $PM_{2.5}/PM_{10}$ ratio highlight the need for targeted pollution control strategies, particularly in areas with high mining activity.

### *4.6. Analysis of Gaseous Air Pollutants*

Figure 18 depicts the gases emitted in the coal mine area, their average concentrations, maximum–minimum values, and their extremely high observations in a box plot. They all have a very high mean compared to the WHO and NAAQS standards. Figure 18 shows that the carbon dioxide ($CO_2$) boxplot shows a narrow range with no visible outliers. The narrow range suggests consistent $CO_2$ levels, possibly due to regular mining activities. The sulfur dioxide ($SO_2$) boxplot has a compact interquartile range (IQR), showing outliers above the upper whiskers. The CO box plot features a larger IQR, and the median is closer to the lower quartile. The levels of $SO_2$ and CO suggest the limited sulfur and incomplete combustion sources in the area. The nitrogen dioxide ($NO_2$) boxplot has an extended upper whisker, indicating variability at higher concentrations, and the median is closer to the lower quartile. The ozone ($O_3$) boxplot has an even longer upper whisker, indicating higher variability at elevated concentrations. Ozone ($O_3$) is formed through complex chemical reactions involving precursor pollutants, such as nitrogen oxides ($NO_x$) and the volatile organic compounds (VOCs) in the presence of sunlight. The relationship between $NO_2$

and $O_3$ is driven by photochemical reactions, where $NO_2$ emitted from combustion sources contributes to the formation of ozone ($O_3$) under sunlight. However, high levels of NO (produced from $NO_2$) can also break down ozone, leading to a dynamic and context-dependent correlation between these pollutants. During the day, when photochemical reactions are most active, the correlation between $NO_2$ and $O_3$ tends to be strong but can fluctuate depending on local emissions and atmospheric conditions. Emissions of $NO_x$ and VOCs from diesel-powered equipment, blasting activities, and natural sources within the mine can contribute to ozone formation through photochemical reactions. Due to their sources and chemical interactions, different pollutants exhibit varying distributions. Monitoring and controlling these pollutants are essential for environmental and public health.

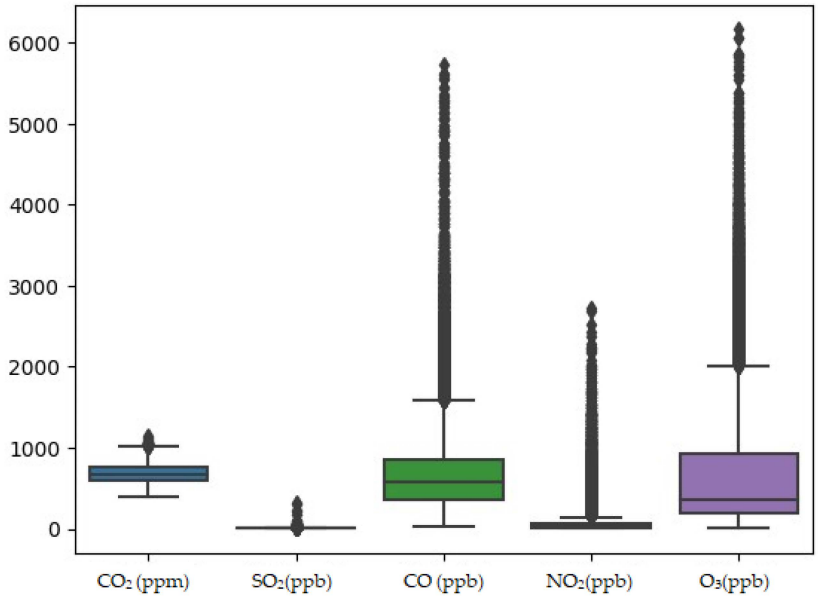


**Figure 18.** Box plots of all gases emitted in the coal mine site.

## 5. Remote Monitoring and Engineering Controls Established

### *5.1. Web and Mobile Application Development*

This research enables mining managers to access data remotely anytime, anywhere. Remote access and analysis of the data are also possible. A web app login and AQI mobile app are available to access the data. The features include accessing data remotely, updates to data in real-time, analytics using historical data, and graphical representations, as shown in Figure 19.

### *5.2. Remedial Measures to Reduce Dust Pollution and Improve Air Quality*

The following engineering controls/measures that can effectively control the air pollution in opencast mines include dust suppression techniques, wet spraying, and dry fog systems. Wet sprays suppress dust during drilling, blasting, and material handling. Dry fog systems are used to suppress dust from mineral processing plants. In addition, planting vegetation around mining areas can serve multiple purposes, such as soil stabilization and trapping dust. Enclosing the conveyor belts, crushers, and other equipment can minimize dust dispersion. Regular maintenance of vehicles and optimizing blasting practices can reduce fragmentation and dust production. Some of the modern technologies that are used in India for air quality management in mines are shown in the figures below (Figures 20–23).

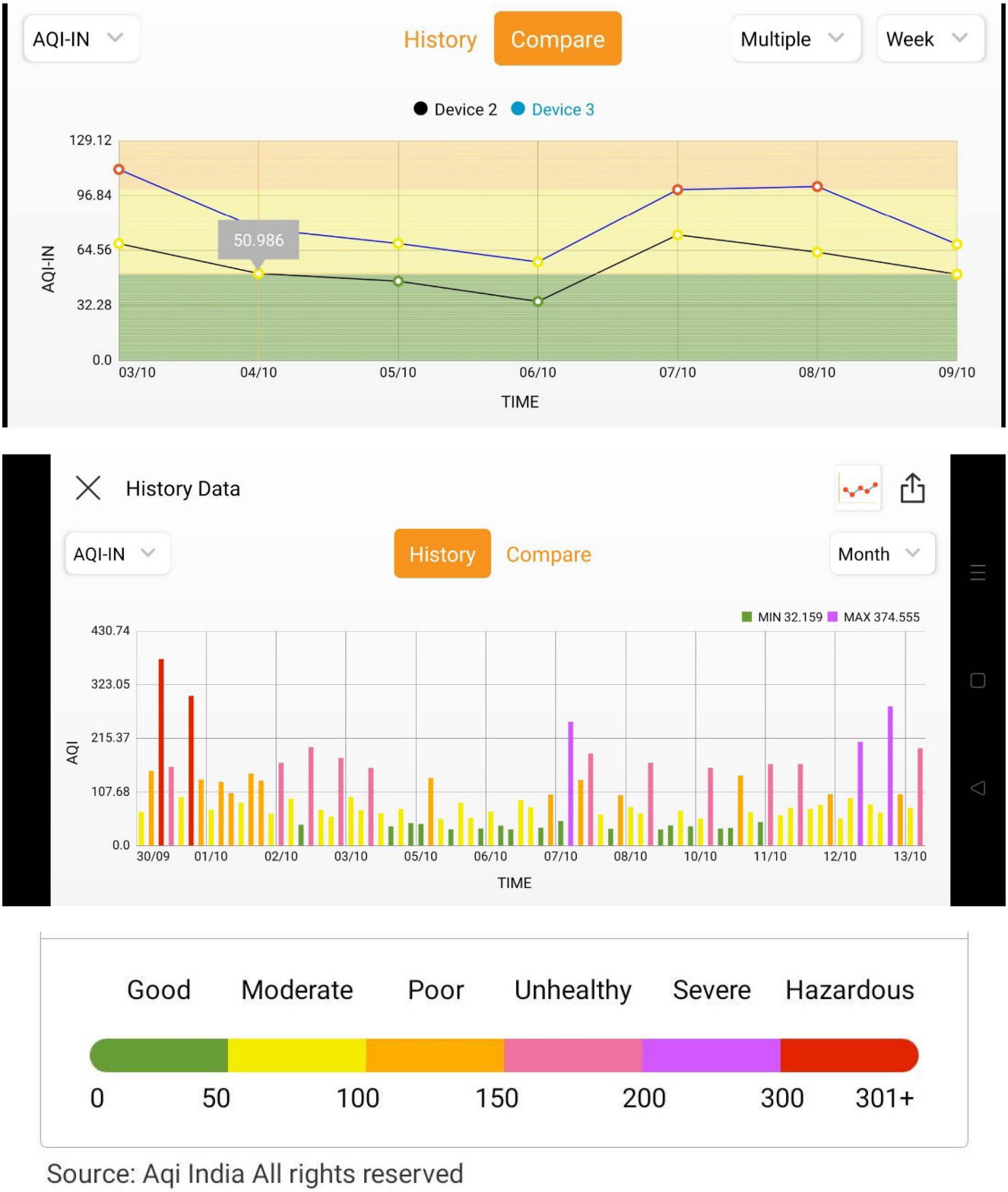


**Figure 19.** Web and Mobile application charts and graphs for visualization of AQI data. two lines indicated two different devices located at two locations and graph indicates the comparison between those two locations.




**Figure 20.** Surface Miner with water jets, Gevra OCP, SECL (Source: Annual report 2023–2024; Ministry of Coal, India).




**Figure 21.** Drill machine with dust extractors (Source: Annual report 2023–2024; Ministry of Coal, India [58]).




**Figure 22.** Air pollution control measures Nigahi OCP, NCL (Source: Annual report 2023–2024; Ministry of Coal, India).




**Figure 23.** Fog canon for dust suppression at Nigahi OC of NCL (Source: Annual report 2023–2024; Ministry of Coal, India).

## 6. Conclusions

This study successfully implemented an IoT and AI-based system for real-time monitoring of particulate matter (PM) and greenhouse gas (GHG) emissions in a surface coal mine. Key findings revealed that PM concentrations were highest at the mine site, with average levels of $PM_{2.5}$ and $PM_{10}$ reaching 159.11 $\mu g/m^3$ and 180.48 $\mu g/m^3$, respectively, significantly exceeding the National Ambient Air Quality Standards (NAAQS) limits. The buffer zone had slightly lower average concentrations of $PM_{2.5}$ (134.75 $\mu g/m^3$) and $PM_{10}$ (153.0 $\mu g/m^3$). By contrast, the IIT–ISM site, located 12 km from the mine, recorded much lower values of 64.33 $\mu g/m^3$ ($PM_{2.5}$) and 74.6 $\mu g/m^3$ ($PM_{10}$), falling within acceptable limits. The air quality index (AQI) averaged 258.97 at the mine site, falling into the "very unhealthy" category, with significant health implications for workers and nearby residents.

A key finding was the effect of meteorological factors on PM levels. The temperature inversion phenomenon, where cool air traps pollutants near the ground, was observed, particularly in the early morning, causing PM concentrations to peak around 6:00 a.m. The correlation between PM levels and temperature was negative, while humidity had a positive correlation, with higher humidity leading to increased PM concentrations. For instance, PM levels rose as temperatures decreased, with the $R^2$ value of 0.45 at the mine site showing a significant relationship between these factors. A major contribution of this research is the development of an integrated command and control center (ICCC), which provides real-time data collection and analysis through low-cost sensors. This system offers actionable insights for pollution control measures, such as optimizing water sprinkling locations and monitoring GHG emissions. While this study achieved significant progress,

there are opportunities for further improvement. The monitoring period was only four months, so we could gather even more valuable insights by extending this study over different seasons to see how air quality changes throughout the year. In conclusion, our study on real-time air pollution monitoring in Indian open-cast coal mines has provided significant insights into the dynamics of particulate matter (PM) in these environments. A notable highlight is the measurement of $PM_1$ in real-time, which sheds light on finer particles that can have substantial health implications. The continuous and cloud-stored data from Indian coal mines, particularly focusing on PM levels, serves as a crucial step towards comprehensive environmental monitoring. Temperature inversion, particle counts, and the cyber-physical systems employed, including mobile and web applications for decision management, contribute to a robust monitoring framework. The analysis of the $PM_{2.5}$ to $PM_{10}$ ratio and the correlation of PM levels with temperature and humidity adds depth to our understanding of air quality dynamics.

Our findings highlight a strong correlation between $PM_{2.5}$, $PM_{10}$, and $PM_1$, emphasizing the interconnected nature of different particulate sizes. Moreover, we have identified production activities as a significant contributor to PM, stressing the need for effective mitigation strategies within the mining sector.

Furthermore, our differentiation of monitoring sites, encompassing actual mines, residential areas, offices, and university campuses, provides a nuanced perspective on air quality variations in diverse settings. This study enhances our comprehension of pollution sources and lays the foundation for targeted interventions and policy formulation to address air quality concerns in and around open-cast coal mines in India.

**Author Contributions:** Conceptualization: V.S.; methodology: V.S.; validation: V.S., S.A. and R.W.; formal analysis: P.J.; investigation: V.S.; resources: V.S.; data curation: P.J.; writing—original draft preparation: V.S.; writing—review and editing: Y.P.C.; visualization: V.S.; supervision: S.A.; project administration: S.A.; funding acquisition: S.A. All authors have read and agreed to the published version of the manuscript.

**Funding:** This research received no external funding. The APC was not funded by any organization.

**Institutional Review Board Statement:** Not applicable. This study did not involve humans or animals and did not require ethical approval.

**Informed Consent Statement:** Not applicable. This study did not involve human.

**Data Availability Statement:** The data presented in this study are available on request from the corresponding author.

**Acknowledgments:** We thank IIT (ISM) for their financial and infrastructure support. We also thank BCCL officials for their invaluable support and collaboration in facilitating this study and permitting us to install instruments. Their assistance has been integral to the successful completion of this research endeavor.

**Conflicts of Interest:** Author Renzhong Wang was employed by the company Microsoft. The remaining authors declare that the research was conducted in the absence of any commercial or financial relationships that could be construed as a potential conflict of interest.

# Appendix A

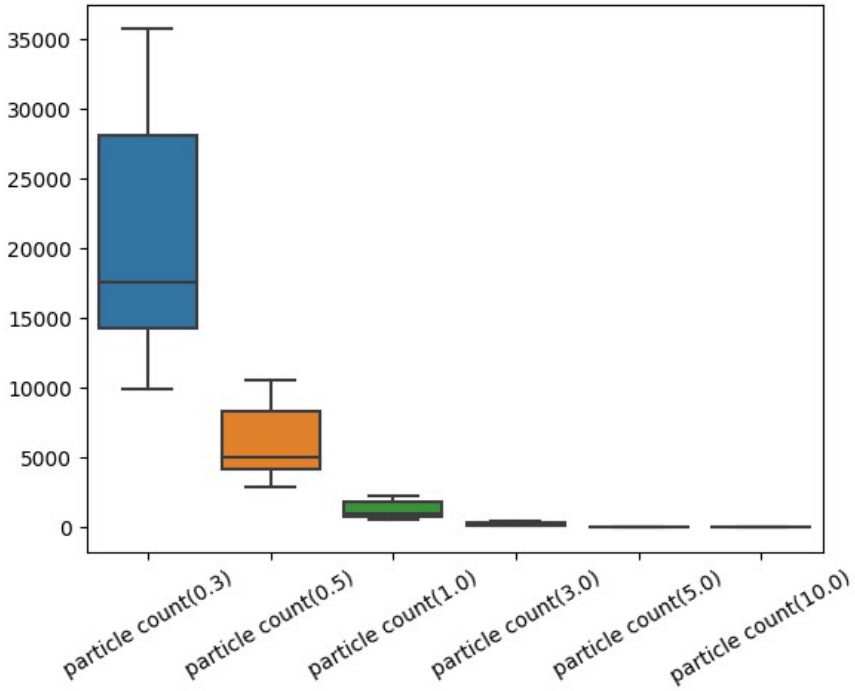


**Figure A1.** The box plot displays the particle count for PM.

**Table A1.** Main Parameters of Air Quality Monitoring Sensor.

| Parameters | Range | Resolution | Accuracy |
|---|---|---|---|
| $PM_{10}$ | 0–2000 μg/m$^3$ | 1 μg/m$^3$ | +/−10%(1–150 μg/m$^3$) |
| $PM_{2.5}$ | 0–2000 μg/m$^3$ | 1 μg/m$^3$ | +/−15% (>150 μg/m$^3$) |
| $PM_1$ | 0–2000 μg/m$^3$ | 1 μg/m$^3$ | +/−15% (>150 μg/m$^3$) |
| $CO_2$ | 1 ppm | 0–10,000 ppm | +/−3.0% |
| $SO_2$ | 10 ppb | 0–20 ppm | +/−3.0%, 50 ppm |
| $NO_2$ | 10 ppb | 0–20 ppm | +/−3.0% |
| $O_3$ | 10 ppb | 0–20 ppm | +/−3.0% |
| CO | 10 ppb | 0–1000 ppm | +/−3.0% |
| Temperature | 20–60 °C | 1 °C | +/−3.0% |
| Humidity | 0–99% | 1% | +/−3.0% |

*Spearman's Rank Analysis*

The mean concentrations of $PM_1$, $PM_{2.5}$, $PM_{10}$, and AQI followed similar trends across all locations during the study period. Spearman's rank analysis was used to determine the correlation between particulate matter of various sizes ($PM_1$, $PM_{2.5,}$ and $PM_{10}$) and AQI [56,59]. For all locations, there is a high positive correlation between AQI with $PM_1$, $PM_{2.5}$, and $PM_{10}$ because the higher the concentrations of PM in the air, the worse the air quality. Therefore, AQI increases as particulate matter increases. There is high negative correlation between PM and temperature at the mine site and the mine office (HQ) locations [60].

At the mine site and the mine office (HQ) locations, there was a strong negative correlation between PM and temperature, with Spearman's coefficients of −0.67 and −0.57, respectively, as shown in Figure A2a,b. At the IIT–ISM location, the correlation between PM and temperature was weakly negative, with a Spearman coefficient of −0.17.

Additionally, there was a moderate positive correlation between PM and humidity at the mine site and the mine office (HQ) locations, with Spearman's coefficients of 0.73 and 0.72, respectively. At the IIT–ISM location, the correlation between PM and humidity was weakly positive [61], as shown in Figure A2c. PM demonstrated a strong correlation with temperature under high humidity conditions (when RH > 50%) but otherwise showed a weak negative correlation with humidity [62].

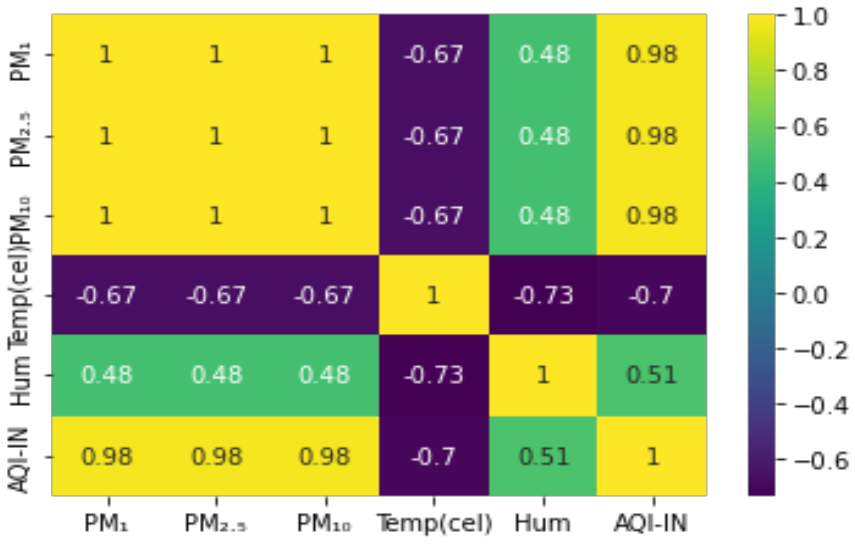


(**a**)

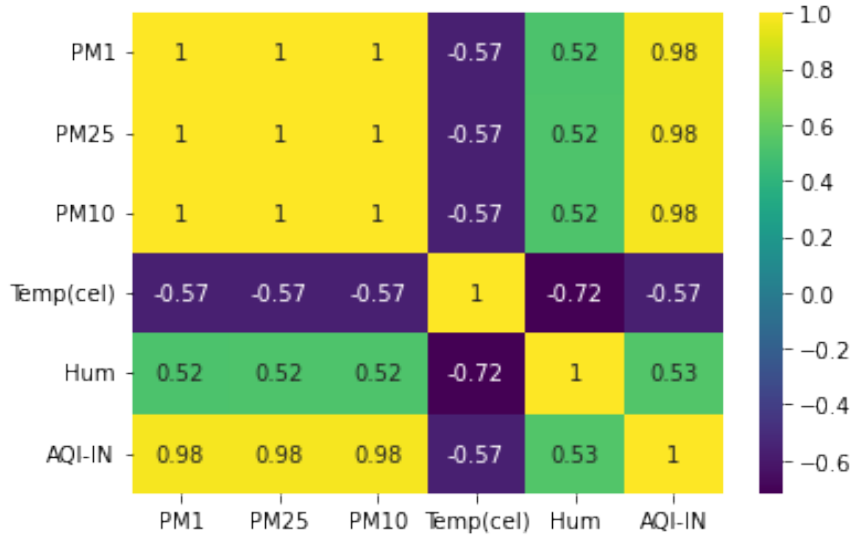


(**b**)

**Figure A2.** *Cont.*

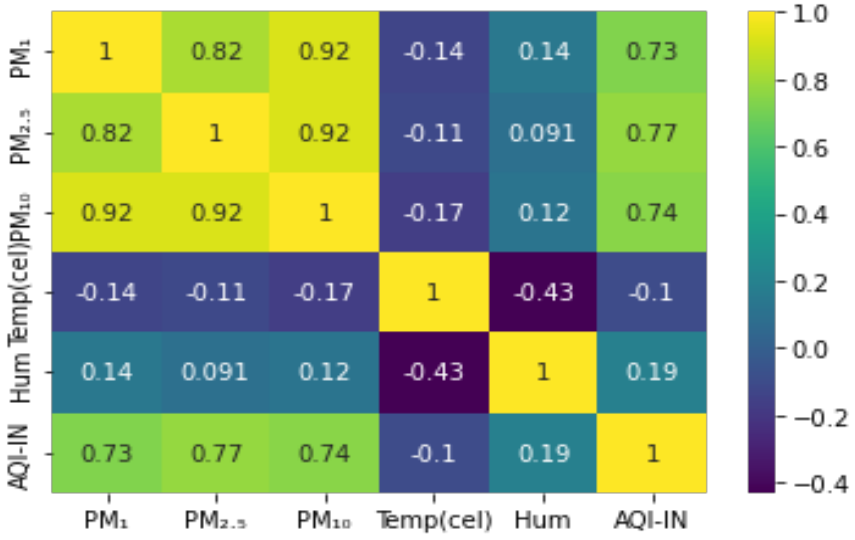


(**c**)

**Figure A2.** Spearman's correlation coefficients for $PM_1$, $PM_{2.5}$, and $PM_{10}$, and AQI, temperature and humidity measured at all three locations. (**a**) Spearman's correlation coefficients for $PM_1$, $PM_{2.5}$, $PM_{10}$, and AQI for temperature and humidity measured at the mine site. (**b**) Spearman's correlation coefficients for $PM_1$, $PM_{2.5}$, $PM_{10}$, and AQI for temperature and humidity measured at the mine office (HQ). (**c**) Spearman's correlation coefficients for $PM_1$, $PM_{2.5}$, $PM_{10}$, and AQI for temperature and humidity measured at the IIT–ISM.

## References

1. Singh, K.; Meena, R.S.; Kumar, S.; Dhyani, S.; Sheoran, S.; Singh, H.M.; Pathak, V.V.; Khalid, Z.; Singh, A.; Chopra, K.; et al. India's renewable energy research and policies to phase down coal: Success after Paris agreement and possibilities post-Glasgow Climate Pact. *Biomass Bioenergy* **2023**, *177*, 106944. [CrossRef]
2. Srikanth, R.; Bhatt, J.R. *Why India Needs Coal to Achieve Its Sustainable Development Goals (No. f6dhe)*; Center for Open Science: Charlottesville, VA, USA, 2023.
3. Mishra, A.; Das, N.; Chhetri, P. Sustainable strategies for the Indian coal sector: An econometric analysis ap-proach. *Sustainability* **2023**, *15*, 11129. [CrossRef]
4. Ministry of Coal Press Information Bureau, India's Coal Production Targets and Achievements, Ministry of Coal, Government of India. 2023. Available online: https://pib.gov.in/PressReleaseIframePage.aspx?PRID=1984997 (accessed on 11 December 2023).
5. Singh, N.P.; Seervi, V.; Kishore, N.; Verma, A.K. Impact of Surface Miner Utilisation on Production Efficiency in Opencast Coal Mines Using Least Squares Method: A Case Study. *J. Inst. Eng. Ser. D* **2024**, *105*, 567–580. [CrossRef]
6. Chen, X.H.; Tee, K.; Elnahass, M.; Ahmed, R. Assessing the environmental impacts of renewable energy sources: A case study on air pollution and carbon emissions in China. *J. Environ. Manag.* **2023**, *345*, 118525. [CrossRef]
7. Sofia, D.; Gioiella, F.; Lotrecchiano, N.; Giuliano, A. Mitigation strategies for reducing air pollution. *Environ. Sci. Pollut. Res.* **2020**, *27*, 19226–19235. [CrossRef]
8. World Health Organization. *WHO Global Air Quality Guidelines: Particulate Matter (PM2.5 and PM10), Ozone, Nitrogen Dioxide, Sulfur Dioxide and Carbon Monoxide*; World Health Organization: Geneva, Switzerland, 2021.
9. Alhajeri, N.S.; Alrashidi, A.M.; Yassin, M.F.; Al-Awadi, L. Optimizing indoor air quality: Investigating particulate matter exposure in household kitchens and source identification. *Environ. Qual. Manag.* **2024**, *34*, 22198. [CrossRef]
10. Roy, A.A.; Adams, P.J.; Robinson, A.L. Air pollutant emissions from the development, production, and processing of Marcellus Shale natural gas. *J. Air Waste Manag. Assoc.* **2014**, *64*, 19–37. [CrossRef]
11. Hosseini, S.H.; Taghizadeh-Alisaraei, A.; Ghobadian, B.; Abbaszadeh-Mayvan, A. Performance and emission char-acteristics of a CI engine fuelled with carbon nanotubes and diesel-biodiesel blends. *Renew. Energy* **2017**, *111*, 201–213. [CrossRef]
12. Zhaglovskaya, A.V.; Savon, D.Y.; Safronov, A.; Sidorova, E. Production activity analysis methodology for open pit coal mines (in terms of Shestaki open pit mine). *Eurasian Min.* **2017**, *1*, 27. [CrossRef]
13. Roy, S.; Adhikari, G.R.; Singh, T.N. Development of Emission Factors for Quantification of Blasting Dust at Surface. *J. Environ. Prot.* **2010**, *1*, 346–361. [CrossRef]
14. Pandey, V.C.; Ahirwal, J.; Roychowdhury, R.; Chaturvedi, R. *Eco-Restoration of Mine Land*; John Wiley & Sons: Hoboken, NJ, USA, 2022.

15. Chaulya, S.; Chowdhury, A.; Kumar, S.; Singh, S.; Singh, R.; Prasad, G.; Mandal, S.; Banerjee, G. Fugitive dust emission control study for a developed smart dry fog system. *J. Environ. Manag.* **2021**, *285*, 112116. [CrossRef] [PubMed]
16. Lashgari, A.; Kecojevic, V. Comparative analysis of dust emission of digging and loading equipment in surface coal mining. *Int. J. Min. Reclam. Environ.* **2015**, *30*, 181–196. [CrossRef]
17. Mondal, S.; Singh, G.; Jain, M.K. Spatio-temporal variation of air pollutants around the coal mining areas of Jharia Coalfield, India. *Environ. Monit. Assess.* **2020**, *192*, 405. [CrossRef] [PubMed]
18. Carlson, C.L.; Adriano, D.C. Environmental Impacts of Coal Combustion Residues. *J. Environ. Qual.* **1993**, *22*, 227–247. [CrossRef]
19. Honscha, L.C.; Penteado, J.O.; Gama, V.D.S.; Bonifácio, A.d.S.; Aikawa, P.; dos Santos, M.; Baisch, P.R.M.; Muccillo-Baisch, A.L.; Júnior, F.M.R.d.S. Health impact assessment of air pollution in an area of the largest coal mine in Brazil. *Environ. Sci. Pollut. Res.* **2021**, *29*, 14176–14184. [CrossRef]
20. Chadwick, M.J.; Lindman, N. (Eds.) *Environmental Implications of Expanded Coal Utilization: A Study by*; The Beijer Institute the United Nations Environment Programme the USSR Academy of Sciences: Stockholm, Sweden; Elsevier: Amsterdam, The Netherlands, 2013.
21. Chakraborty, M.; Ahmad, M.; Singh, R.; Pal, D.; Bandopadhyay, C.; Chaulya, S. Determination of the emission rate from various opencast mining operations. *Environ. Model. Softw.* **2002**, *17*, 467–480. [CrossRef]
22. Huertas, J.; Huertas, M.; Cervantes, G.; Díaz, J. Assessment of the natural sources of particulate matter on the opencast mines air quality. *Sci. Total Environ.* **2014**, *493*, 1047–1055. [CrossRef]
23. Oliveira, M.L.; Akinyemi, S.A.; Nyakuma, B.B.; Dotto, G.L. Environmental impacts of coal nanoparticles from rehabilitated mine areas in Colombia. *Sustainability* **2022**, *14*, 4544. [CrossRef]
24. Trechera, P.; Moreno, T.; Córdoba, P.; Moreno, N.; Zhuang, X.; Li, B.; Li, J.; Shangguan, Y.; Dominguez, A.O.; Kelly, F.; et al. Comprehensive evaluation of potential coal mine dust emissions in an open-pit coal mine in Northwest China. *Int. J. Coal Geol.* **2021**, *235*, 103677. [CrossRef]
25. Candeias, C.; Ávila, P.; Coelho, P.; Teixeira, J.P. Mining activities: Health impacts. In *Reference Module in Earth Systems and Environmental Sciences*; Springer: Berlin/Heidelberg, Germany, 2018; pp. 1–21.
26. Patra, A.K.; Gautam, S.; Kumar, P. Emissions and human health impact of particulate matter from surface mining operation—A review. *Environ. Technol. Innov.* **2016**, *5*, 233–249. [CrossRef]
27. Hendryx, M.; Islam, M.S.; Dong, G.-H.; Paul, G. Air Pollution Emissions 2008–2018 from Australian Coal Mining: Implications for Public and Occupational Health. *Int. J. Environ. Res. Public Health* **2020**, *17*, 1570. [CrossRef] [PubMed]
28. Gautam, S.; Prasad, N.; Patra, A.K.; Prusty, B.K.; Singh, P.; Pipal, A.S.; Saini, R. Characterization of $PM_{2.5}$ generated from opencast coal mining operations: A case study of Sonepur Bazari Opencast Project of India. *Environ. Technol. Innov.* **2016**, *6*, 1–10. [CrossRef]
29. Wang, J.; Ogawa, S. Effects of meteorological conditions on PM2.5 concentrations in Nagasaki, Japan. *Int. J. Environ. Res. Public Health* **2015**, *12*, 9089–9101. [CrossRef] [PubMed]
30. Manisalidis, I.; Stavropoulou, E.; Stavropoulos, A.; Bezirtzoglou, E. Environmental and health impacts of air pollution: A review. *Front. Public Health* **2020**, *8*, 14. [CrossRef] [PubMed]
31. Li, G.; Koomson, D.A.; Huang, J.; Amponsah, E.I.; Darkwah, W.K.; Miwornunyuie, N.; Li, K.; Dong, X. A review from environmental management to environmental governance: Paradigm shift for sustainable mining practice in Ghana. *Environ. Dev. Sustain.* **2021**, *23*, 9710–9724. [CrossRef]
32. Hansen, J.; Sato, M.; Russell, G.; Kharecha, P. Climate sensitivity, sea level and atmospheric carbon dioxide. *Philos. Trans. R. Soc. A Math. Phys. Eng. Sci.* **2013**, *371*, 20120294. [CrossRef]
33. Zhou, S.; He, H.; Zhang, L.; Zhao, W.; Wang, F. A Data-Driven Method to Monitor Carbon Dioxide Emissions of Coal-Fired Power Plants. *Energies* **2023**, *16*, 1646. [CrossRef]
34. Erhan, L.; Ndubuaku, M.; Di Mauro, M.; Song, W.; Chen, M.; Fortino, G.; Bagdasar, O.; Liotta, A. Smart anomaly detection in sensor systems: A multi-perspective review. *Inf. Fusion* **2021**, *67*, 64–79. [CrossRef]
35. Nižetić, S.; Šolić, P.; González-de-Artaza, D.L.-D.I.; Patrono, L. Internet of Things (IoT): Opportunities, issues and challenges towards a smart and sustainable future. *J. Clean. Prod.* **2020**, *274*, 122877. [CrossRef]
36. Liu, X.; Bai, S.; Yuan, J.; Sun, H. Intelligent Monitoring and Management System for Coal Mines Using Internet of Things Technology. In Proceedings of the Innovative Computing, Taichung, Taiwan, 23–26 January 2024; Pei, Y., Ma, H.S., Chan, Y.-W., Jeong, H.-Y., Eds.; Springer: Singapore, 2024.
37. Kim, S.-M.; Choi, Y.; Suh, J. Applications of the Open-Source Hardware Arduino Platform in the Mining Industry: A Review. *Appl. Sci.* **2020**, *10*, 5018. [CrossRef]
38. Sharma, R.; Kumar, A. Analysis of seasonal and spatial distribution of particulate matters and gaseous pollutants around an open cast coal mining area of Odisha, India. *Environ. Sci. Pollut. Res.* **2023**, *30*, 39842–39856. [CrossRef] [PubMed]
39. Jiang, Y.; Chen, W.; Zhang, X.; Zhang, X.; Yang, G. Real-Time Monitoring of Underground Miners' Status Based on Mine IoT System. *Sensors* **2024**, *24*, 739. [CrossRef] [PubMed]

40. Medina, F.; Ruiz, H.; Espíndola, J.; Avendaño, E. Deploying IIoT Systems for Long-Term Planning in Underground Mining: A Focus on the Monitoring of Explosive Atmospheres. *Appl. Sci.* **2024**, *14*, 1116. [CrossRef]
41. Molaei, F.; Rahimi, E.; Siavoshi, H.; Afrouz, S.G.; Tenorio, V. A Comprehensive Review on Internet of Things (IoT) and its Implications in the Mining Industry. *Am. J. Eng. Appl. Sci.* **2020**, *13*, 499–515. [CrossRef]
42. Zhang, H.; Li, B.; Karimi, M.; Saydam, S.; Hassan, M. Recent Advancements in IoT Implementation for Environmental, Safety, and Production Monitoring in Underground Mines. *IEEE Internet Things J.* **2023**, *10*, 14507–14526. [CrossRef]
43. Kundu, S.; Pal, A.K. Application of AERMOD model in air quality ($PM_{10}$) impact assessment of selected opencast mines in The Jharia Coalfield, Jharkhand, India. *Environ. Prot. Eng.* **2018**, *44*, epe180401. [CrossRef]
44. Naik, A.S.; Reddy, S.K.; Raj, M.G. RTEPMS: Real Time Environmental Parameters Monitoring System using IoT based LoRa 868 MHz Wireless Communication Technology in Underground Mines. *IEEE Access* **2024**, *12*, 3350429. [CrossRef]
45. Giordano, M.R.; Malings, C.; Pandis, S.N.; Presto, A.A.; McNeill, V.; Westervelt, D.M.; Beekmann, M.; Subramanian, R. From low-cost sensors to high-quality data: A summary of challenges and best practices for effectively calibrating low-cost particulate matter mass sensors. *J. Aerosol Sci.* **2021**, *158*, 105833. [CrossRef]
46. Alfano, B.; Barretta, L.; Del Giudice, A.; De Vito, S.; Di Francia, G.; Esposito, E.; Formisano, F.; Massera, E.; Miglietta, M.L.; Polichetti, T. A Review of Low-Cost Particulate Matter Sensors from the Depvelopers' Perspectives. *Sensors* **2020**, *20*, 6819. [CrossRef]
47. Ayele, T.W.; Mehta, R. Air pollution monitoring and prediction using IoT. In Proceedings of the 2018 Second International Con-Ference on Inventive Communication and Computational Technologies (ICICCT), Coimbatore, India, 20–21 April 2018; IEEE: Piscataway, NJ, USA, 2018; pp. 1741–1745.
48. Manikandan, S.V.; Abilash, Y.; Prasanth, S.H.; Daniel, J.A.; Santhosh, R. Internet of things enabled ml for air quality assessment: Systematic review. In Proceedings of the 2023 7th International Conference on Intelligent Computing and Control Systems (ICICCS), Madurai, India, 17–19 May 2023; IEEE: Piscataway, NJ, USA, 2023; pp. 1509–1514.
49. Tsiompra, M. Early Warning System for Monitoring Air Pollution Using an IoT Platform. Ph.D. Thesis, Aristotle University of Thessaloniki, Thessaloniki, Greece, 2023.
50. NAAQS_2019, National Ambient Air Quality Standards (NAAQS) Annual Report 2019. Central Pollution Control Board. Available online: http://www.cpcb.nic.in/ (accessed on 18 October 2024).
51. Ghose, M.K.; Majee, S.R. Air Pollution due to Opencast Coal Mining and It's Control in Indian Context. *J. Sci. Ind. Res.* **2001**, *60*, 786–797.
52. Bulletin of Ambient Air Quality National Ambient Air Quality Monitoring Programme (NAMP)-Manual Monitoring System. Central Pollution Control Board Ministry Of Environment, Forests & Climate Change. 2016. Available online: http://www.cpcb.nic.in/ (accessed on 18 October 2024).
53. Ghose, M.K.; Majee, S.R. Assessment of Dust Generation Due to Opencast Coal Mining—An Indian Case Study. *Environ. Monit. Assess.* **2000**, *61*, 257–265. [CrossRef]
54. Sinha, S.; Banerjee, S. Characterization of haul road dust in an Indian opencast iron ore mine. *Atmos. Environ.* **1997**, *31*, 2809–2814. [CrossRef]
55. Sastry, V.R.; Chandar, K.R.; Nagesha, K.V.; Muralidhar, E.; Mohiuddin, M.S. Prediction and analysis of dust dispersion from drilling operation in opencast coal mines. *Procedia Earth Planet. Sci.* **2015**, *11*, 303–311. [CrossRef]
56. Hernandez, G.; Berry, T.A.; Wallis, S.; Poyner, D. Temperature and humidity effects on particulate matter concentrations in a sub-tropical climate during winter. *Int. Proc. Chem. Biol. Environ. Eng.* **2017**, *102*, 41–49.
57. Liu, L.Y.; Ji, H.G.; Lü, X.F.; Wang, T.; Zhi, S.; Pei, F.; Quan, D.L. Mitigation of greenhouse gases released from mining activities: A review. *Int. J. Miner. Metall. Mater.* **2021**, *28*, 513–521. [CrossRef]
58. Ministry of Coal. *Annual Report 2023–2024*; Ministry of Coal: New Delhi, India, 2024.
59. Tripathi, A.K.; Aruna, M.; Gowripathi Rao, N.R.N.V.; Ray, S. Design and Development of an IoT-Based Gas Monitoring System for Underground Coal Mines. In *Recent Trends in Mechanical Engineering: Select Proceedings of PRIME 2021*; Springer: Berlin/Heidelberg, Germany, 2023; pp. 489–495.
60. Kirešová, S.; Guzan, M. Determining the correlation between particulate matter $PM_{10}$ and meteorological factors. *Eng* **2022**, *3*, 343–363. [CrossRef]
61. Onuorah, C.U.; Leton, T.G.; Momoh, Y.O.L. Influence of Meteorological Parameters on Particle Pollution ($PM_{2.5}$ and $PM_{10}$) in the Tropical Climate of Port Harcourt, Nigeria. *Arch. Curr. Res. Int.* **2019**, *19*, 1–12. [CrossRef]
62. Vaishali; Verma, G.; Das, R.M. Influence of Temperature and Relative Humidity on $PM_{2.5}$ Concentration over Delhi. *MAPAN* **2023**, *38*, 759–769. [CrossRef]


**Disclaimer/Publisher's Note:** The statements, opinions and data contained in all publications are solely those of the individual author(s) and contributor(s) and not of MDPI and/or the editor(s). MDPI and/or the editor(s) disclaim responsibility for any injury to people or property resulting from any ideas, methods, instructions or products referred to in the content.